SWEDISH GEOTECHNICAL INSTITUTE

PROCEEDINGS
No. 23

STRENGTH AND DEFORMATION PROPERTIES OF SOILS AS DETERMINED BY A FREE FALLING WEIGHT

By
Olle Orrje & Bengt Broms

STOCKHOLM 1970

SWEDISH GEOTECHNICAL INSTITUTE
PROCEEDINGS
No. 23

STRENGTH AND DEFORMATION PROPERTIES OF SOILS AS DETERMINED BY A FREE FALLING WEIGHT

By
Olle Orrje & Bengt Broms

STOCKHOLM 1970

PREFACE

The research work presented in this report was performed at the Division of Soil Mechanics of the Royal Institute of Technology and the Swedish Geotechnical Institute, Stockholm, by Tekn. lic. Olle Orrje (1968), under the supervision of Dr. Bengt B. Broms, Director of the Swedish Geotechnical Institute. It was supported by a grant from the Swedish National Council of Building Research (Statens Råd för Byggnadsforskning, Stockholm).

Stockholm, March 1970
SWEDISH GEOTECHNICAL INSTITUTE

CONTENTS

SUMMARY

The strength-deformation properties of cohesionless soils (sands) under dynamic loading have in the present investigation been determined by measuring the retardation of a free falling weight when it strikes the surface of a soil mass. The reaction force on the weight has been calculated from Newton's second law and the penetration of the weight into the underlying soil by intergrating twice the retardation-time relationships with respect to time. The load-deformation relationships as determined by this method have been compared with those from static load tests.

The test results indicate that the dynamic load-deformation relatioships are affected mainly by the dry unit weight of the sand and that a free falling weight can be used to check the relative density and the degree of compaction of a particular soil.

1. INTRODUCTION

The purpose of the present study was to investigate the dynamic strength and deformation properties of compacted cohesionless soils (sands) by measuring the retardation of a free falling weight (Fig. 1) and to determine if these properties can be used as an indication of the relative density of a soil (Orrje, 1968). This method was first proposed by Forssblad (1963, 1965 and 1967).

The dynamic strength-deformation properties of soils have previously been investigated by e.g. Taylor & Whitman (1954). Dynamic load tests have also been carried out by Selig & McKee (1961), Shenkman & McKee (1961), Cunny & Sloan (1961), Fisher (1962), White (1964) and Vesić, Banks & Woodard (1965).

In the calculation of settlements and deformations of cohesionless soils an equivalent modulus of elasticity E of the soil is often used. This modulus is generally evaluated by static plate load tests (static method) or from the seismic velocity of the soil (dynamic method). Static plate load tests give only an indication of the value of the local equivalent modulus of elasticity within a depth which corresponds to two plate diameters.

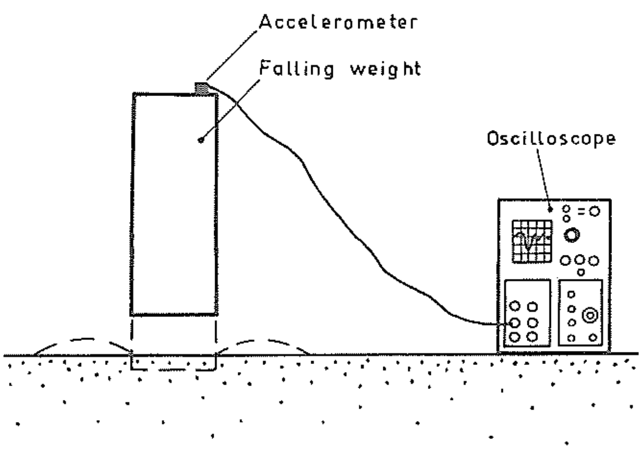

Fig. 1 Load test with a free falling weight

The modulus of elasticity calculated from the seismic velocity is an average value for a relatively large volume of soil. This modulus is generally much higher than the equivalent modulus obtained from load tests. It is therefore of interest to know the relation between static strength and deformation properties of different soils and the corresponding dynamic values at different loading rates and loading intensities. Comparisons are made in

---

For translation of the English units in this report the following values are to be used:

1 in.	=	2.54 cm
1 ft^2	=	929 cm^2
1 lb	=	0.45 kg
1 lb/ft^3	=	0.016 kg/dm^3
1 ton/ft^2	=	0.98 kp/cm^2

this report between values of the modulus of elasticity and the failure loads obtained from static plate load tests on cohesionless soils (sand) and the corresponding dynamic values from load tests with free falling weights. The investigation includes both laboratory and field tests. Also the different failure modes and the depth to which the different load tests affected the underlying soil have been investigated. The height of the free fall, the size of the loaded area, the mass of the weight and the degree of compaction of the underlying soil were varied.

2. SOIL MATERIALS

Three types of sand were investigated. These are in this report called G 12 Sand, Baskarp Sand and Örsholm Sand.

G 12 Sand which is a beach sand of marine origin with rounded particles has a grain size distribution as shown in Fig. 2. It can be seen that the sand is well sorted with a low coefficient of uniformity ($C_u = \frac{d_{60}}{d_{10}} = 2.08$). This sand has been used in numerous laboratory investigations at the Danish Geotechnical Institute, e.g. by Hansen & Odgaard (1960) and Christensen (1961).

The Baskarp Sand consists mainly of subrounded quartz particles with the grain size distribution as shown in Fig. 2. The average grain size is larger, and the coefficient of uniformity ($C_u = 3.75$) higher than that of the G 12 Sand.

The grain size distribution of the Örsholm Sand used in the field tests is also shown in Fig. 2. This sand had been dredged from the river Klarälven and placed at the test site in the summer of 1966, approximately one year before the tests. The thickness of the sand layer was approximately 10 ft. The sand surface was levelled by a tractor before the tests.

The minimum void ratio e_{min} of the three sands was determined by the modified Proctor compaction test with owen dried material and the maximum void ratio e_{max} by pouring dry sand through a funnel into a Proctor mould. The tip of the funnel was held at the sand surface in the mould. The results are shown in Table 1.

The angle of internal friction of the three sands was determined by triaxial tests with owen dried samples at a confining pressure of 22.5 psi. In Fig. 3 is shown the angle of internal friction φ

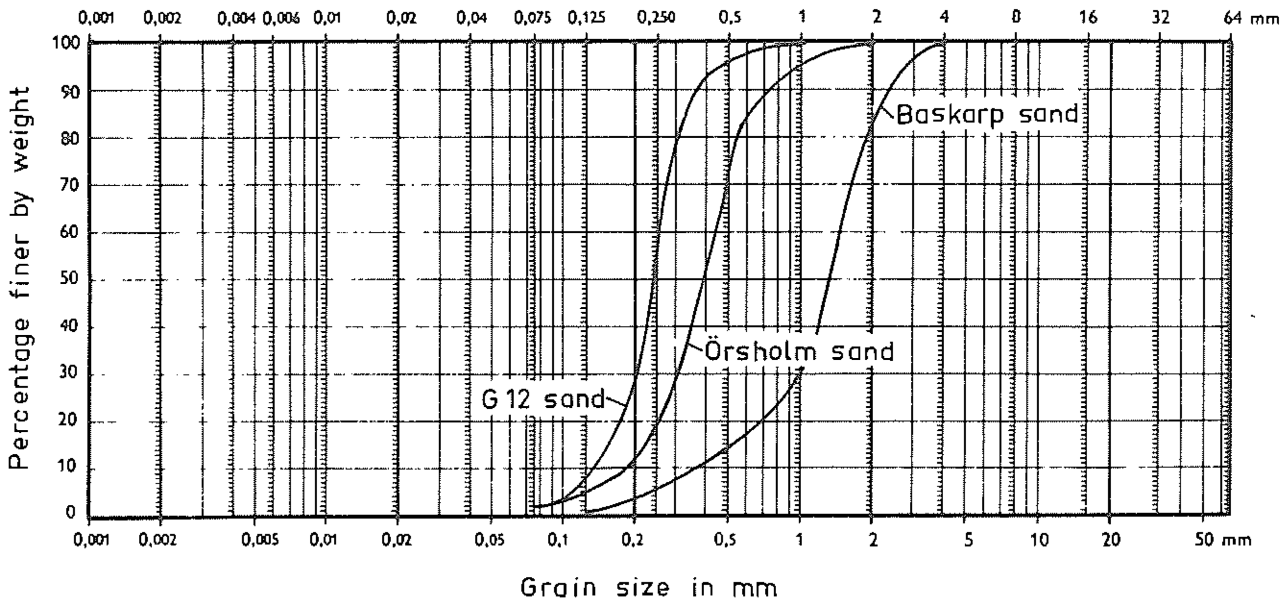

Fig. 2 Grain size distribution

TABLE 1. Index Properties of Soils Tested

Type of Sand	Unit Weight of Solids γ_s lb/ft^3	Min Void Ratio e_{min}	Max Void Ratio e_{max}	Max Dry Unit Weight γ_{max} lb/ft^3	Min Dry Unit Weight γ_{min} lb/ft^3	Uniformity Coefficient C_u
G 12 Sand	165.3	0.590	0.839	104.0	90.0	2.08
Baskarp Sand	165.6	0.471	0.642	112.5	101.0	3.75
Örsholm Sand	165.4	0.574	0.822	105.5	97.0	2.25

obtained from the triaxial tests, as a function of the porosity n of the sands. The relationships are approximately linear and it can be seen that the Baskarp Sand has a higher angle of internal friction than the Örsholm or the G 12 Sand. Hansen & Odgaard (1960) obtained in their triaxial tests slightly higher values of φ for the G 12 Sand than those shown in Fig. 3 obtained in the present investigation.

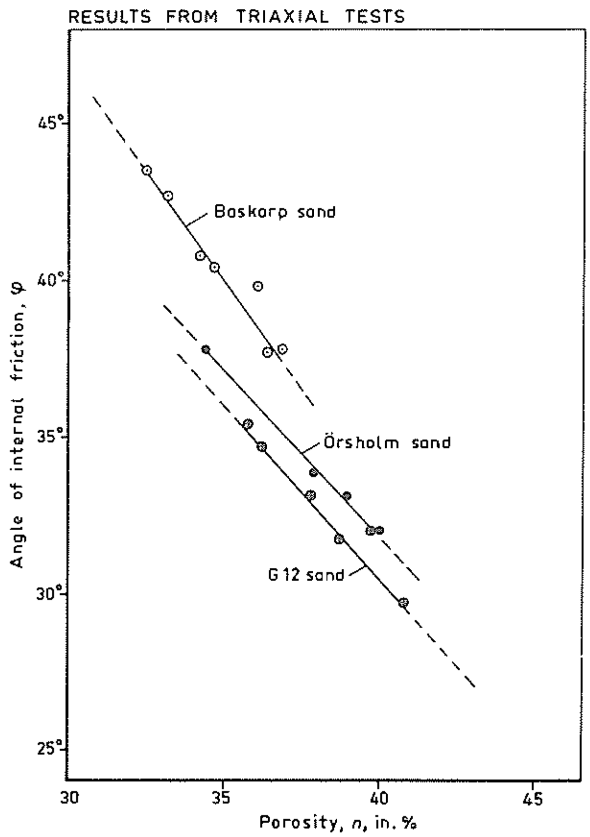

Fig. 3 Triaxial tests on G12, Örsholm and Baskarp Sands

3. TEST ARRANGEMENTS AND PREPARATION

3.1 Test program

<u>Static Load Tests.</u> Seven static test series were carried out numbered 1-7. The parameters investigated in the different series are given in Table 2.

The failure load, the equivalent modulus of elasticity and the bearing capacity factors N_{γ}^{stat} and N_{q}^{stat} have been calculated from the results obtained in each test, as described in the previous section.

TABLE 2. Test Results from Static Laboratory and Field Tests

Test No.	Dry Unit Weight γ lb/ft^3	Void Ratio e	Poro-sity $n\%$	Angle of Internal Friction φ^o	Diame-ter of Plate B in.	Failure Load P_{ult}^{stat} lbs	Average Pressure at Failure σ_{ult}^{stat} tons/ft^2	Equivalent Modulus of Elasticity E_{eq}^{stat} tons/ft^2
Laboratory Tests					G 12 Sand			
1a:a	107.5	0.543	35.2	35.8	6	401	1.05	8.9
1a:b						373	0.98	9.4
1b:a					4	104	0.61	4.2
1b:b						112	0.66	3.5
1c:a					2	11.2	0.26	-
1c:b						13.9	0.33	-
2a:a	106.3	0.562	36.0	34.9	6	319	0.83	8.7
2a:b						350	0.92	8.1
2b:a					4	95.0	0.56	5.0
2b:b						83.0	0.49	4.0
2c:a					2	12.1	0.28	1.4
2c:b						10.8	0.25	3.3
3a:a	105.0	0.576	36.5	34.3	6	195.1	0.51	5.3
3a:b						200.0	0.52	5.4
3b:a					4	84.8	0.50	3.5
3b:b						81.2	0.48	3.7
3c:a					2	9.2	0.21	-
3c:b						-	-	-
4a:a	103.1	0.604	37.7	33.0	6	195	0.55	5.7
4a:b						241	0.63	5.7
4b:a					4	107	0.63	4.2
4b:b						86.5	0.51	4.3
4c:a					2	9.9	0.23	-
4c:b						7.3	0.17	-
5a:a	101.5	0.644	39.2	31.4	6	140	0.37	5.2
5a:b						128	0.34	3.9
5b:a					4	46.7	0.27	3.2
5b:b						38.1	0.22	2.8
5c:a					2	12.1	0.28	-
5c:b						-	-	-
					Baskarp Sand			
6a:a	113.2	0.466	31.8	44.4	6	672	1.76	17.6
6a:b						692	1.81	22.5
6b:a					4	104	0.61	5.7
6b:b						105	0.62	5.7
6c:a					2	12.1	0.28	-
6c:b						13.0	0.30	-
Field Tests					Örsholm Sand			
7a:a	96.3	0.78	44.0		4	211	1.24	14.0
7a:b						224	1.33	13.5
7b:a					6	550	1.45	14.3
7b:b						487	1.27	12.6
7c:a					12	2270	1.49	54.1
7c:b						1960	1.28	27.5
7d:a					24	-	-	57.0
7d:b						-	-	36.1
7d:c						-	-	27.6

Dynamic Load Tests. The investigation included eight test series where the mass of the falling weight, the height of free fall, the diameter of the striking bottom plate surface of the weights and the dry unit weight of the sands were varied (see Table 3).

TABLE 3. Test Results from Dynamic and Static Load Tests

Test No.	Dry Unit Weight γ lb/ft^3	Void Ratio e	Porosity n%	Mass of Weight m lb	Height of Free Fall h_o in.	Diameter of Plate B in.	Total Penetration δ in.	Equivalent Modulus of Elasticity E^{dyn}_{eq} tons/ft^2	E^{stat}_{eq} tons/ft^2	Contact Pressure at Failure σ^{dyn}_{ult} tons/ft^2	σ^{stat} tons/ft^2
					G 12 Sand						
A:1a	107.5	0.543	35.2	203.5	2	6	0.71	21.6	9.2	2.32	0.90
A:1b							0.71	18.8		2.16	1.16
A:2a					4		1.15	21.6	9.2	2.74	1.12
A:2b							1.15	23.9		2.51	1.23
A:3a					8		1.83	23.8	9.2	2.96	1.15
A:3b							-	-		2.85	1.27
A:4a					16		3.35	41.4		3.25	1.02
A:4b							3.35	32.4		3.25	1.00
B:1a	106.3	0.562	36.0	203.5	2	6	0.99	13.9	8.4	1.77	1.09
B:1b							0.95	14.7		1.85	1.08
B:2a						4	3.22	5.8	4.5	1.67	0.77
B:2b							-	-		-	-
B:3a						2	3.98	5.9	1.8	1.45	0.45
B:3b							3.98	-		-	-
C:1a	105.0	0.576	36.5	203.5	2	6	1.11	11.4	5.4	1.60	0.99
C:1b							1.35	10.8		1.59	0.95
C:2a				428			1.83	9.0	5.4	2.65	1.04
C:2b							1.83	12.2		2.79	0.92
C:3a				1100			3.98	9.0	5.4	2.71	0.82
C:3b							-	-		-	-
C:4a	103.1	0.604	37.7	203.5	2	6	1.63	9.2	5.7	1.44	0.98
C:4b							1.91	8.0		1.41	1.07
C:5a				428			3.39	10.8	5.7	1.45	0.82
C:5b							2.59	-		-	-
C:6a	101.5	0.644	39.2	203.5	2	6	1.79	11.7	4.5	1.20	0.90
C:6b							1.91	9.0		1.18	0.87
C:7a				428			3.98	9.2	4.5	1.25	0.84
C:7b							3.98	11.5		1.37	0.94
D:1a	103.8	0.595	37.4	203.5			1.83	8.0	-	1.45	-
D:1b							2.07	6.8		1.40	-
D:2a	106.9	0.548	35.3				0.81	14.6	9.2	1.91	1.16
D:2b							0.91	14.6		1.87	1.16
					Baskarp Sand						
E:1a	113.2	0.466	31.8	203.5	2	6	1.59	29.3	19.9	2.59	1.41
E:1b							-	-		-	-
E:2a				428			2.63	12.7	19.9	2.45	1.87
E:2b							2.71	-		-	-
E:3a				1100			3.98	20.5	19.9	2.49	1.86
E:3b							3.98	20.7		2.98	1.96
					Örsholm Sand						
F:1a	96.3	0.78	44	203.5	2	6	1.08	15.1	13.5	2.33	1.93
F:1b							1.08	14.8	13.5	2.00	1.87
F:2a	98.2	0.75	43		4		1.49	14.4	13.5	2.71	2.20
F:2b							1.54	18.0	13.5	2.83	2.21
F:3a	97.6	0.76	43		8		2.15	14.0	13.5	2.97	2.27
F:3b							2.23	18.2	13.5	3.12	2.19
F:4a	96.8	0.78	44		16		3.30	20.7	13.5	3.49	2.69
F:4b							3.26	24.2	13.5	3.63	2.65
G:2a	95.0	0.80	44	203.5	2	4	2.46	8.7	13.8	1.65	1.20
G:2b							2.39	6.3	13.8	1.67	1.20
H:2a	98.2	0.73	42	428	2	6	1.99	14.0	13.5	3.18	2.50
H:2b							1.59	17.9	13.5	3.45	2.22

3.2 Compaction of Sand for Laboratory Tests

The sand was placed in the wooden box by pouring it in layers through a flexible rubber hose. The layer thickness was decreased from approximately 3 in. at the bottom of the container to approximately 0.8 in. at the top. Each layer was compacted by a tamper which was allowed to fall freely from a height of approximately 8 in. The weight of the tamper was 7.6 lbs and the diameter of the circular bottom plate of the tamper was 6.0 in. The number of blows for each layer was varied in order to obtain a constant density of the sands throughout the container.

The dry unit weight of the compacted sand was determined in both the laboratory and field tests by the drive cylinder method. A thin walled cylinder with 3.75 in. inside diameter and 5.2 in. height was used in these experiments.

3.3 Static Laboratory Tests

The test arrangement for the static laboratory plate load tests is shown in Figs. 4 and 5. The tests were carried out in a rigid rectangular wooden box which was placed directly on a concrete floor and had the dimensions 4.3 x 4.3 x 1.65 ft. The diameters of the plates used at the load tests were 2.0, 4.0 and 6.0 in., and the bottom of the plates were grooved to provide a rough contact surface with the underlying soil. The minimum distance from the edge of the loading plates to the side of the container was 12.0 in. Two parallel load tests were carried out after the sand had been placed and compacted to check the reproducibility of the test results.

The plates were loaded by a hydraulic jack. The displacement rate in all static tests was 0.4 in./min. The applied load was measured by a load cell (Bofors KRG-4 500 kp) and the penetration by a displacement transducer (Sanborn 7 DC DT 3000) while the load-settlement curves were recorded by an x-y recorder (type Mosely 7030 AM).

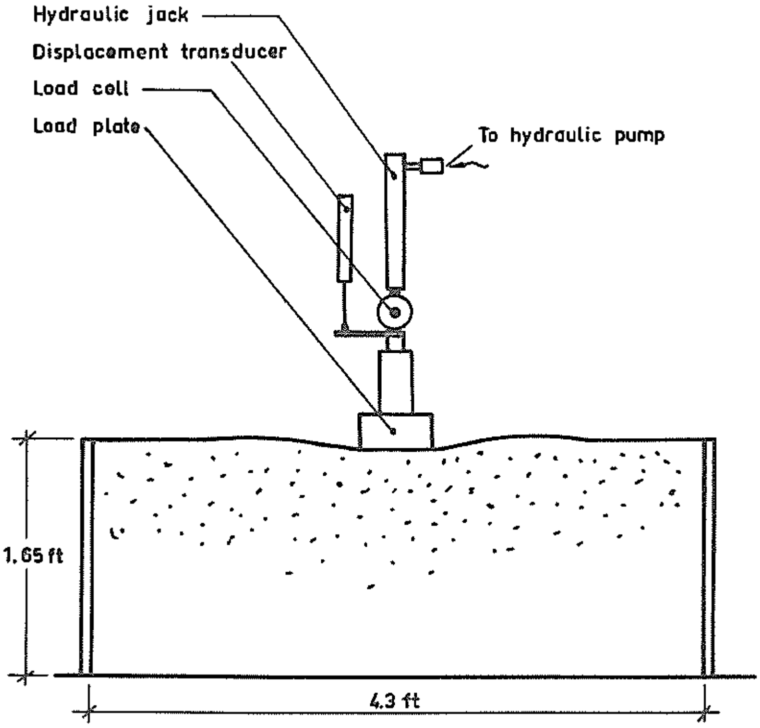

Fig. 4 Test arrangement for static load tests (in principle)

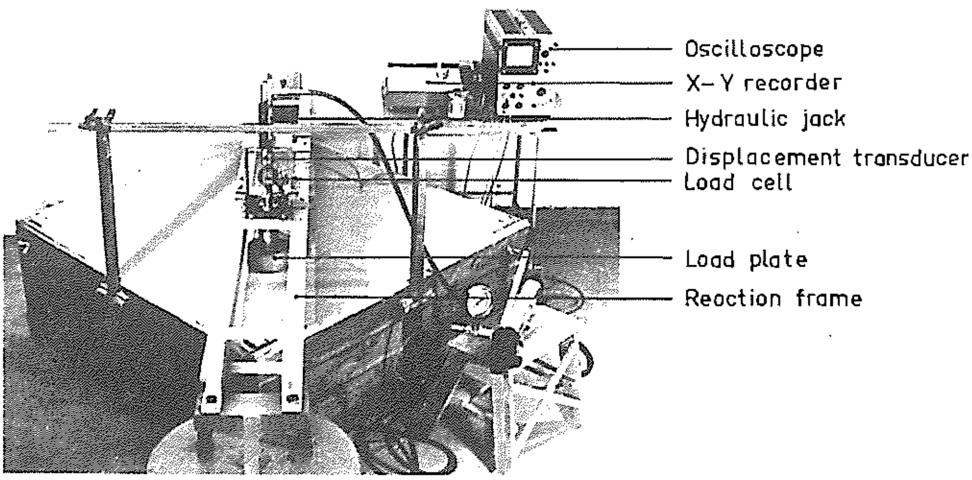

Fig. 5 View of experimental arrangement for static laboratory load tests

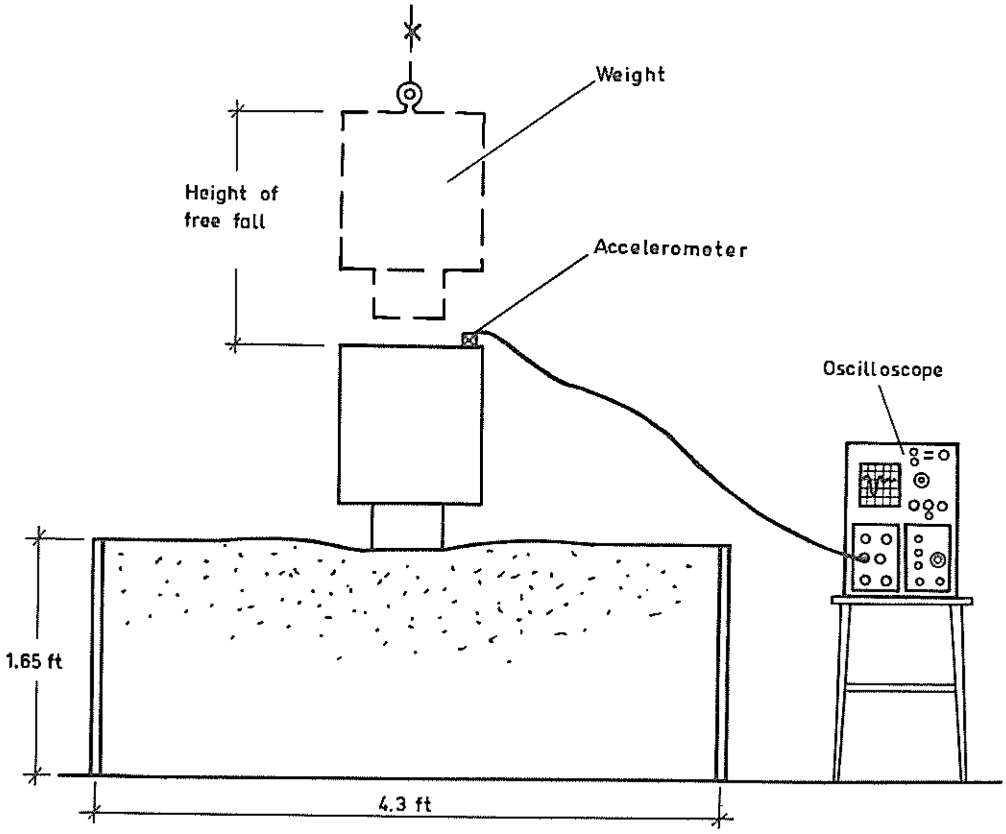

Fig. 6 Test arrangement for dynamic load tests

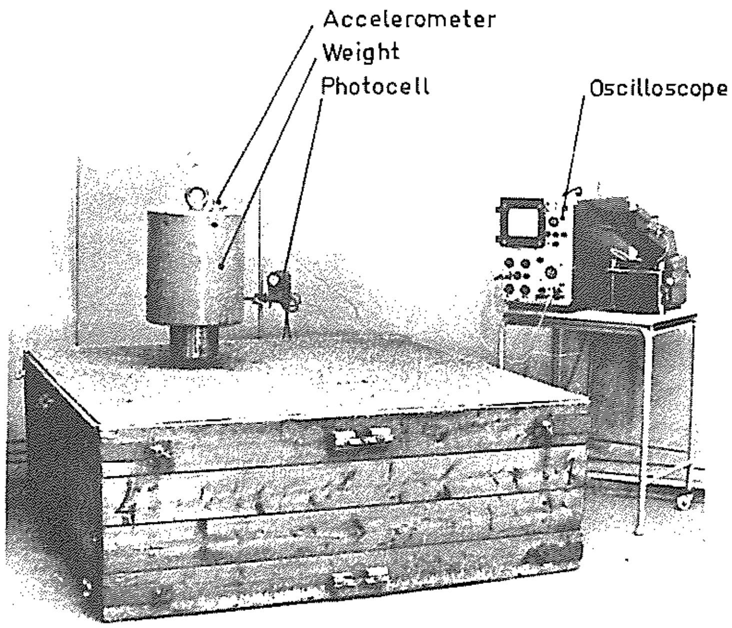

Fig. 7 View of experimental arrangement for dynamic laboratory load tests

3.4 Dynamic Laboratory Tests

The test arrangement for the dynamic laboratory tests is illustrated in Figs. 6 and 7. The mass of the falling weight which was used in these tests was 203.5, 428 and 1 100 lbs, respectively. The diameter of the bottom surface of the weight was also varied (2.0, 4.0 and 6.0 in.). The height of free fall (2, 4, 8 and 16 in.) was controlled by a thin steel wire. The weights were released by cutting the wire with a pair of pliers.

The retardation of the falling weight when it struck the sand surface was measured by an accelerometer (Model CEC type 4-202-0129) which was rigidly attached to the weight. The signals from the accelerometer were registered by an oscilloscope (Tektronix Type 564 with plugin units 2B67 and 3C66). A photocell was used to trigger the oscilloscope as can be seen in Fig. 7, und the obtained retardation-time curves were photographed by a polaroid camera (Tektronix C-12).

3.5 Static Field Tests

Plates with 4, 6, 12 and 24 in. diameter were used for the static field load tests. The load was applied by a hydraulic jack mounted on a truck. The deformation rate was 0.4 in./min. The applied load was measured by a load cell (Bofors, LSK-2 2000 kp) and the settlements by a displacement transducer (Sanborn 7 DC DT 3 000), while the load-settlement relationships were registered by an x-y recorder (Mosely 7030 AM).

3.6 Dynamic Field Tests

For these tests the same testing equipment was used as for dynamic laboratory tests and the mass of the falling weight was 203.5 and 428 lbs, respectively. The diameter of the circular bottom surface of the weights was 4 or 6 in.

4. INTERPRETATION OF TEST RESULTS

4.1 Static Load Tests

Failure Load. The overburden pressure at the bottom of a loaded plate increases when the plate is pushed into the soil. The corresponding increase of the bearing capacity of the plate can be determined from the shape of the load-settlement curve as shown in Fig. 8. It can be seen from this figure that the initial part of the curve is approximately straight. When the failure is approached, the settlement (penetration) of the loaded plate increases rapidly with increasing applied load. The load-settlement curves generally have a sharp break when the relative density of the sand is high, while the slope changes more gradually when the relative density is low.

After the failure load has been exceeded, there is a further increase of the bearing capacity of the plates with increasing penetration. This part of the load-settlement curve is also approximately straight. The angle β shown in Fig. 8 indicates the effect of the overburden pressure on the failure load. This effect has been taken into account by extrapolating the last straight part of the load settlement curves (dotted line), as shown in Fig. 8. The intercept of the extrapolated part of the curve with the vertical load axis is in this report defined as the static failure load.

Bearing Capacity Factors N_q^{stat} and N_γ^{stat}. The failure stress σ_{ult}^{stat} for a vertically loaded plate placed on sand can theoretically be evaluated as the sum of the two following terms

$$\sigma_{ult}^{stat} = 1/2\, F_\gamma\, \gamma B\, N_\gamma^{stat} + F_q\, q\, N_q^{stat} \qquad (1)$$

where γ is the unit weight of the sand, q the overburden pressure at the bottom of the plate, B the plate diameter, N_γ^{stat} and N_q^{stat} are so called bearing-capacity factors which are only dependent of the angle of internal friction of the soil, and F_γ and F_q are shape-factors which are dependent of the shape of the loaded plate. Load tests indicate that $F_q = 1.2$ and $F_\gamma = 0.6$ are valid for circular plates, Meyerhof (1951), Hansen (1961), Feda (1961). These values have been used in the calculations in this report.

From the results obtained in the static load tests, numerical values of the bearing-capacity factor N_γ^{stat} have been evaluated using Eq. (1). The failure loads defined in Fig. 8 were then used in the calculations.

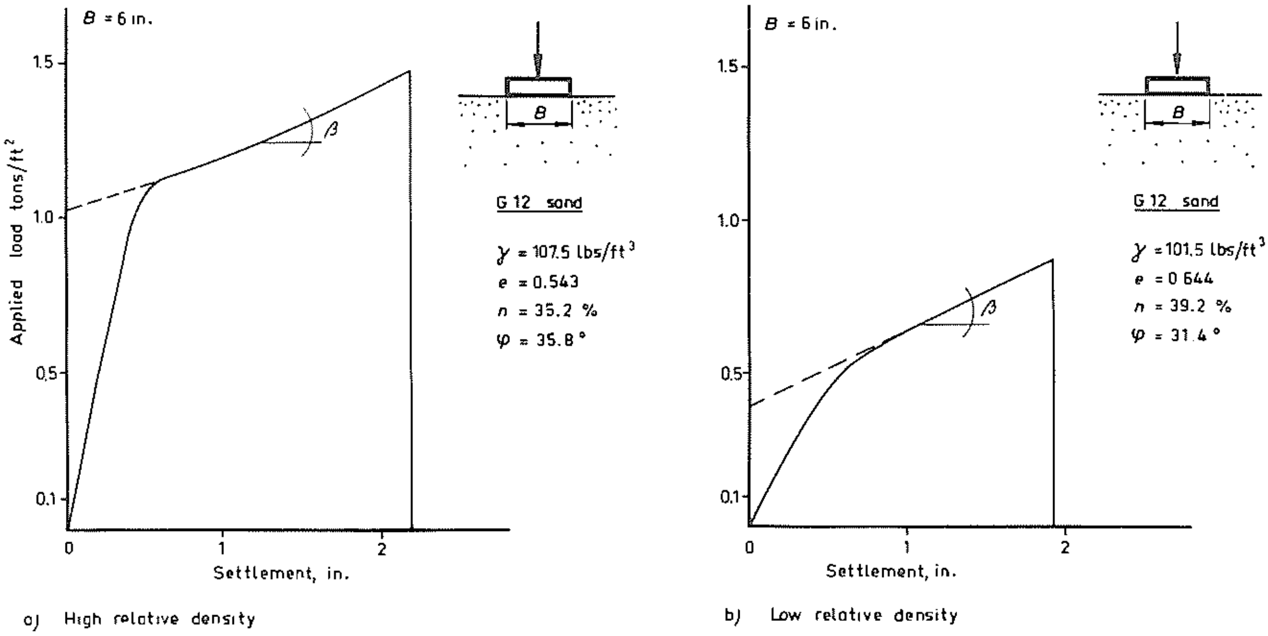

Fig. 8 Interpretation of static load tests

Theoretical values of the bearing-capacity factor N_{γ}^{stat} have been evaluated by Terzaghi (1943), Meyerhof (1951), Lundgren & Morthensson (1953) and others. These calculations show that the numerical values of N_{γ}^{stat} and N_{q}^{stat} are about the same.

Numerical values of the bearing-capacity factor N_{q}^{stat} have also been evaluated from the obtained test results. The slope β of the straight part discussed above of the load settlement curve beyond the failure load (see Fig. 8) has then been used. This increase of the bearing-capacity reflects the effect of an increasing overburden pressure q as mentioned above (the overburden pressure q is equal to $\delta\gamma$, where δ is the settlement of the plate and γ the unit weight of the soil).

The bearing capacity factor N_{q}^{stat} can be calculated theoretically from an assumed failure surface. For a spiral-shaped failure surface it can be shown that

$$N_{q}^{stat} = e^{\pi \tan\varphi} \tan^2 (45^o + \frac{\varphi}{2}) \qquad (2)$$

where φ is the angle of internal friction of the soil.

Equivalent Modulus of Elasticity. An equivalent modulus of elasticity of the compacted sands (E_{eq}^{stat}) has been calculated from the static plate load tests, using the initial straight part of the load settlement curves (Fig. 8). The following equation has been used in the analysis.

$$\delta = \frac{3\pi}{8} \frac{\sigma_m r_o}{E_{eq}^{stat}} \qquad (3)$$

where r_o is the radius of the plate and σ_m is the average contact pressure at a displacement δ of 0.2 in.

Using Eq. (3) it has been assumed that the underlying soil behaves as an ideal elastic, isotropic and semi-infinite material. These assumptions imply that the soil can resist the very high contact pressures which theoretically develop along the edge of a loaded plate, while in reality these pressures cause the soil to yield locally along the perimeter. High tensile stresses develop also theoretically in an ideal elastic material at the surface close to the perimeter of a loaded plate. Since sand has no tensile strength, the real stress distribution will thus not be the same as that in the theoretical case.

An additional factor which for sands also affects the calculated values of an equivalent modulus of elasticity is the size of the loaded area. In reality, the modulus of elasticity of cohesionless materials generally increases with increasing confining pressure and thus with increasing depth below the ground surface. An equivalent modulus for sand calculated by Eq. (3) will therefore be dependent of the plate size and will increase with increasing plate diameter as pointed out by e.g. Terzaghi (1955).

4.2 Dynamic Load Tests

Load-Settlement Relationships. A typical retardation-time relationship obtained from the tests on the G 12 Sand is shown in Fig. 9. The mass of the falling weight and the height of the free fall were in this case 203.5 lbs and 2 in., respectively. The diameter of the striking bottom surface of the weight was 6 in. As can be seen in the figure the time required for the weight to stop from the moment it strikes the soil surface is approximately 100 msec.

For each test the velocity of the weight and the penetration into the underlying soil was calculated by intergrating numerically the obtained retardation-time curve as shown in Fig. 10 and Table 4.

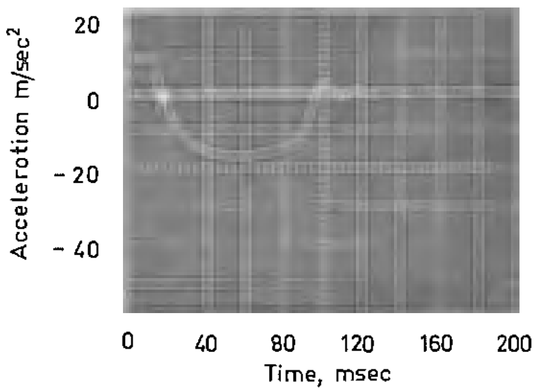

Fig. 9 Retardation-time curve for laboratory test C:4a

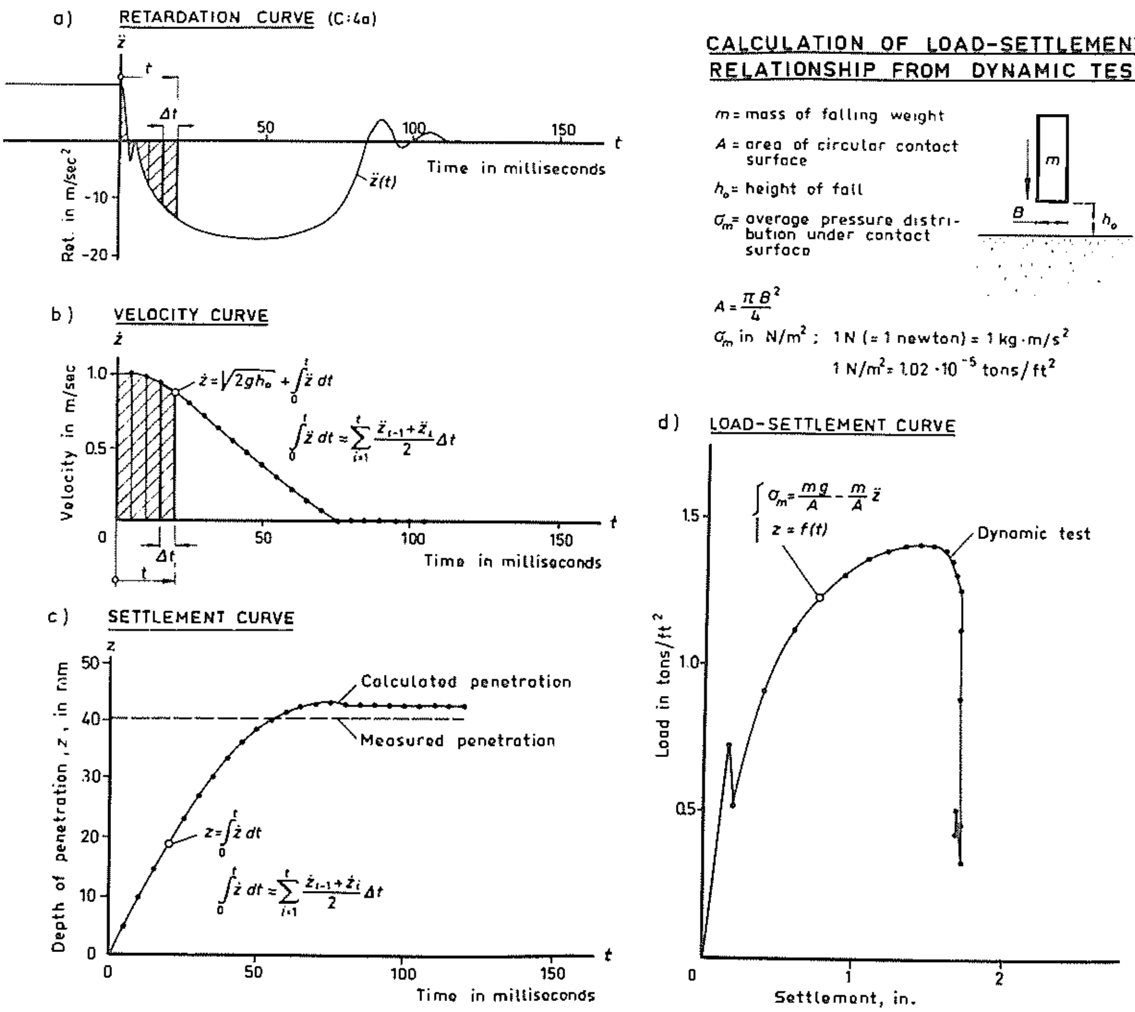

Fig. 10 Calculation of load-settlement relationship from dynamic test C:4a

TABLE 4. Example: Calculation of Load-settlement Relationship from Dynamic Load Test (C:4a)

1 Time t msec	2 Retardation $\ddot{z}$ m/sec^2	3 Integration of Retardation $\frac{\ddot{z}_{i-1}+\ddot{z}_i}{2}\Delta t$	4 Velocity $\dot{z}$ m/sec	5 Integration of Velocity $\frac{\dot{z}_{i-1}+\dot{z}_i}{2}\Delta t$	6 Settlement z mm	7 Average Pressure $\sigma_m \cdot 10^{-4}$ N/m^2
0	9.81		0.9905		0	
4	- 4.0	0.0116	1.0021	3.985	3.99	7.25
5	0.0	0.0020	1.0001	4.980	4.98	5.15
10	- 7.5	0.0188	0.9813	4.953	9.93	9.10
15	- 11.5	0.0475	0.9338	4.788	14.72	11.20
20	- 13.5	0.0625	0.8713	4.513	19.23	12.25
25	- 15.0	0.0713	0.8000	4.178	23.41	13.04
30	- 16.0	0.0775	0.7225	3.808	27.22	13.57
35	- 16.5	0.0813	0.6412	3.410	30.63	13.83
40	- 17.0	0.0838	0.5574	2.998	33.63	14.09
45	- 17.0	0.0850	0.4724	2.575	36.21	14.09
50	- 17.0	0.0850	0.3874	2.149	38.36	14.09
55	- 16.7	0.0843	0.3031	1.726	40.09	13.93
60	- 16.0	0.0818	0.2213	1.311	41.40	13.57
65	- 15.0	0.0775	0.1438	0.913	42.31	13.04
70	- 14.0	0.0725	0.0713	0.538	42.85	12.51
75	- 11.5	0.0638	0.0075	0.197	43.05	11.20
80	- 7.0	0.0463	-0.0388	-0.078	42.93	8.83
85	1.0	0.0150	-0.0538	-0.023	42.91	4.63
90	3.5	0.0113	-0.0425	-0.024	42.89	3.31
95	- 1.5	0.0050	-0.0375	-0.020	42.87	4.36
100	0.0	-0.0030	-0.0405	-0.019	42.85	5.15
105	1.5	0.0030	-0.0375	-0.019	42.83	4.36
110	0.0	0.0030	-0.0345	-0.018	42.81	5.15
115	0.0	0	-0.0345	-0.017	42.79	5.15
120	0.0	0	-0.0345	-0.017	42.77	5.15

m = 203.5 lb　　G 12 Sand

h_o = 2 in.　　γ = 103.1 lb/ft^3

B = 6 in.

The reaction force $\sigma_m A$ from the sand on the weight can thus be calculated from Newton's second law.

$$mg - \sigma_m A = m\ddot{z} \tag{4}$$

where g is the acceleration due to gravity, σ_m the average contact pressure, A the area of the circular striking part of the free falling weight with the mass m, and $\ddot{z}$ the acceleration. This equation can be rewritten as

$$\sigma_m = \frac{mg}{A} - \frac{m}{A}\ddot{z} \tag{5}$$

If the acceleration $\ddot{z}$ is measured with an accelerometer, the average contact pressure σ_m under the weight during the loading can be calculated from the equation

$$\sigma_m = K_1 - K_2\ddot{z} \tag{6}$$

where $K_1 = \frac{mg}{A}$ and $K_2 = \frac{m}{A}$

The penetration z of the falling weight into the sand during the dynamic loading can be calculated by integrating the retardation-time relationship twice with respect to time. The first integration will give the velocity of the weight (Fig. 10 b) according to the equation

$$\int_0^t \ddot{z}dt = z(t) - z(o) \tag{7}$$

while the penetration z of the falling weight into the soil (Fig. 10 c) is obtained after one additional integration

$$z = \int_0^t \dot{z}dt \tag{8}$$

The integrals $\int_0^t \ddot{z}dt$ and $\int_0^t \dot{z}dt$ have in this report been evaluated numerically using the following relationships

$$\int_0^t \ddot{z}dt = \sum_{i=1}^{t} \frac{\ddot{z}_{i-1} + \ddot{z}_i}{2} \Delta t \tag{9}$$

and

$$\int_0^t \dot{z}dt = \sum_{i=1}^{t} \frac{\dot{z}_{i-1} + \dot{z}_i}{2} \Delta t \tag{10}$$

The contact pressure σ_m as a function of the penetration depth z has been obtained from the two relationships $\sigma_m = f(t)$ and $z = f(t)$ as shown in Fig. 10 d.

Failure Load. The dynamic failure load has in this investigation been defined as the applied load which corresponds to the maximum point on the dynamic load-settlement curve. This load has then been compared with the corresponding static load at the same settlement.

Bearing-Capacity Factors N_γ^{dyn} and N_q^{dyn}. Bearing-capacity factors (N_γ^{dyn} and N_q^{dyn}) have been calculated from the dynamic load tests in the same way as for the static tests. In the interpretation of the test results it has been assumed that N_γ^{dyn} is equal to N_q^{dyn}. Thus $N_\gamma^{dyn} = N_q^{dyn} = N_s^{dyn}$. The shape factors F_γ and F_q in Eq. (1) have been assumed to be equal to 0.6 and 1.2, respectively. This will lead to the expression

$$N_s^{dyn} = \frac{\sigma_{ult}^{dyn}}{1/2\ 0,6\,\gamma B + 1,2\,\gamma\delta_f} \tag{11}$$

where δ_f is the penetration of the weight into the soil at failure and γ is the unit weight of the soil.

Equivalent Modulus of Elasticity. A dynamic equivalent modulus of elasticity E_{eq}^{dyn} has been calculated from the dynamic load-settlement curves using Eq. (3).

5. OBTAINED STRENGTH AND DEFORMATION PROPERTIES OF THE SANDS

5.1 Static Load Tests

The results from the static load tests are summarized in Tahle 2.

Failure Load. The obtained failure loads from the static tests were well defined when the relative density of the sand was high. The results from the tests on G 12 Sand agreed also well with those reported by Hansen & Odgaard (1960). (The tests by Hansen & Odgaard were carried out with the same sand and with approximately the same plate diameters as those used in the present investigation.)

Bearing Capacity Factor N_q^{stat}. The values of the bearing-capacity factor N_q^{stat} as calculated by Eq. (1) are shown in Fig. 11 as a function of the angle of internal friction φ of the sand. It can be seen that these experimentally determined values are considerably higher than those calculated theoretically by Eq. (1).

Bearing Capacity Factor N_γ^{stat}. The bearing-capacity factor

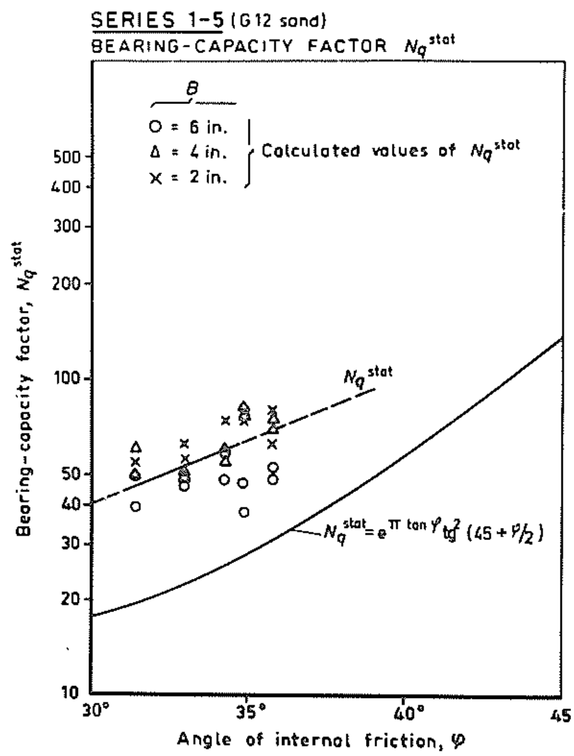

Fig. 11 Results from static load tests - Bearing capacity factor N_q^{stat} as a function of φ .

N_{γ}^{stat} determined by Eq. (1) is shown in Fig. 12 as a function of the friction angle ϕ together with the theoretically calculated values by the method proposed by Meyerhof (1951). The measured values of N_{γ}^{stat} are also considerably higher than the corresponding theoretical values. Similar differences have been reported by Muhs (1954, 1959, 1963), Schultze (1955), Hansen (1961), De Beer & Ladanyi (1961) and Feda (1961).

Several hypotheses have been proposed to explain this difference between theoretical and measured values of N_{γ}^{stat} and N_{q}^{stat}. The difference has for example been attributed to differences in the angle of internal friction of the sand at different values of the intermediate principal stress and at different stress intensities.

Tests by Cornforth (1964) and Bishop (1966) indicate that the angle of internal friction which corresponds to the condition of plane strain is larger than that determined by triaxial tests. Christensen (1961) found for the G12 Sand, which also is used in the present investigation, that the angle of internal friction φ at plane strain is approximately 15 % larger than that determined by triaxial tests. The implication of this difference is that the test points shown in Figs. 11 and 12 should be moved to the right, a distance which corresponds to an increase of the angle of internal friction of approximately 4^{o} when the relative density of the sand is low and approximately 6^{o} when the relative density is high. These corrections will bring the measured values of N_{γ}^{stat} approximately in agreement with the theoretically calculated values.

It could also here be of interest to compare the results obtained in this investigation with relatively small plates, with the results obtained from tests with larger plates. Muhs (1963) has attributed at least part of the difference in behaviour between large and small plates to progressive failure.

According to Muhs the shear strength of soil is first mobilized at the points where the shear stress is the highest. The failure zone spreads gradually from these points to other parts of the soil and when the soil is deformed, its shear strength changes. For an initially loose sand the shear strength and the relative density increases with increasing deformation. Due to this change the failure load will not correspond to the shear strength of the initially undisturbed soil.

The reverse occurs in a sand with a high initial relative density. The relative density and the shear strength of a soil decreases locally with increasing penetration of the loaded plate. Therefore the shear strength of the soil at failure will not correspond

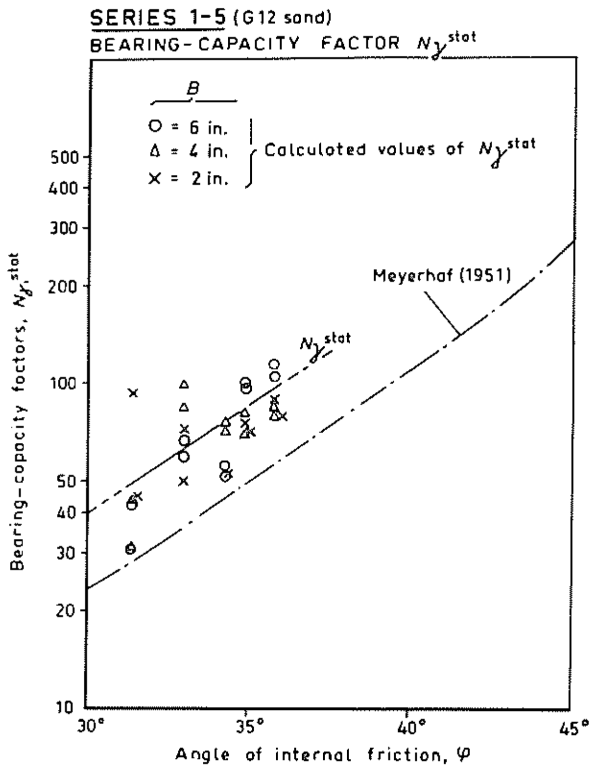

Fig. 12 Results from static load tests - Bearing capacity factor N_{γ}^{stat} as a function of φ.

to the shear strength of the initially dense soil. The failure load will in this case be lower than the theoretically calculated values.

As the displacement required to reach failure increases with increasing plate diameter as pointed out by De Beer & Vesić (1958) and by Vesić (1963), the effects of progressive failure will increase with increasing plate diameter.

As a conclusion, the results by Muhs indicate that it is difficult to correct with a scale factor the bearing-capacity factors determined from tests with relatively small plates, so that they can be used when calculating the bearing-capacity for full scale plates.

<u>Equivalent Modulus of Elasticity</u>. The equivalent modulus of elasticity (E_{eq}^{stat}) has been calculated from Eq. (3), and the values are shown in Table 2. It can be seen that the values from the tests with plates with relatively small diameters (2, 4 and 6 in.) were considerably smaller than those determined from plates with relatively large diameter (12 and 24 in.).

5.2 Dynamic Load Tests

The results from the dynamic tests are summarized in Table 3. In this table are also shown as a comparison, the values of E_{eq}^{stat} and the failure loads from the corresponding static load tests.

Height of Free Fall (h_o). The height of free fall was varied in test series A and F (Table 3). Retardation-time curves obtained with h_o equal to 2, 4, 8 and 16 in. are shown in Figs. 13 and 14.

Three different types of retardation peaks could be observed in the tests. The first of these peaks was observed for series A only in test A:2b, where the height of free fall was 4.0 in., and it occurred approximately 3 msec after the weight struck the surface. This peak could be eliminated by scarifying the soil surface before each test to allow the air to escape which otherwise might be trapped under the weight.

A second retardation peak occurred approximately 5 msec after the weight struck the sand surface and was probably caused by reflection of the compression wave at the bottom of the container. The calculated velocity of the compression wave is about 650 ft/sec, which is approximately equal to the values reported by Lawrence (1961), Whitman & Lawrence (1963) and by Hardin & Richard (1963) for dry sand at low confining pressures.

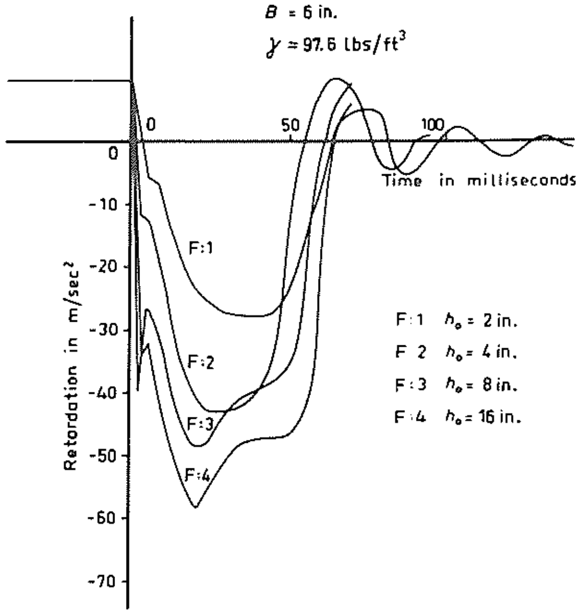

Fig. 14 Retardation-time curves from test series F on Örsholm sand

Since the magnitude of this second retardation peak increased with increasing height of free fall, the height of free fall was reduced to 2 in. in test series B, C and D (Table 3) in order to prevent interference.

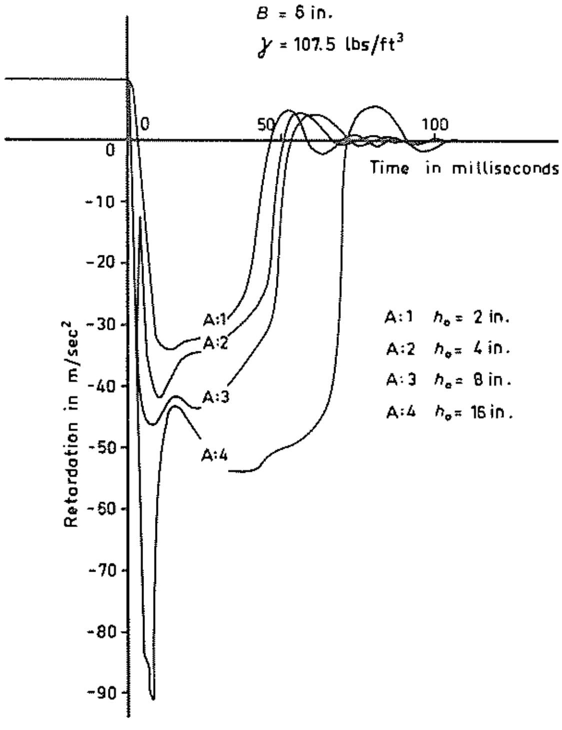

Fig. 13 Retardation-time curves from test series A on G12 sand

As shown in Fig. 13 a third retardation peak occurred approximately 20 to 40 msec after the weight struck the surface. Up to a height of 8 in. the maximum value of this peak increased with increasing of free fall. When the height increased from 8 to 16 in., the increase of the peak value was small.

The dynamic failure loads in each test as calculated from the third retardation peak are shown in Table 3 and Fig. 15. In this figure is also shown the loads from the static load tests which correspond to the settlement at the failure loads of the dynamic load tests. It can be seen that the dynamic failure loads increased with increasing height of free fall and were approximately twice the corresponding static loads.

The values of E_{eq}^{dyn} obtained in test series A are shown in Fig. 16. The values increased with increasing height of free fall, and when the height of free fall is small (2, 4 and 8 in.), the values are almost three times the static values. At a height of 16 in., the values from the dynamic tests are approximately four times the static values.

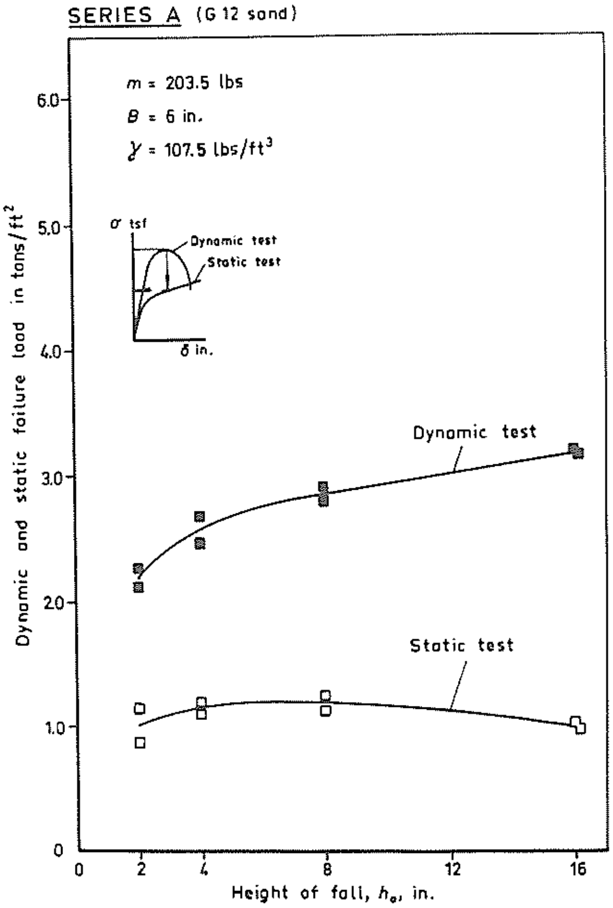

Fig. 15 Dynamic failure load as a function of height of free fall. Test series A and 1

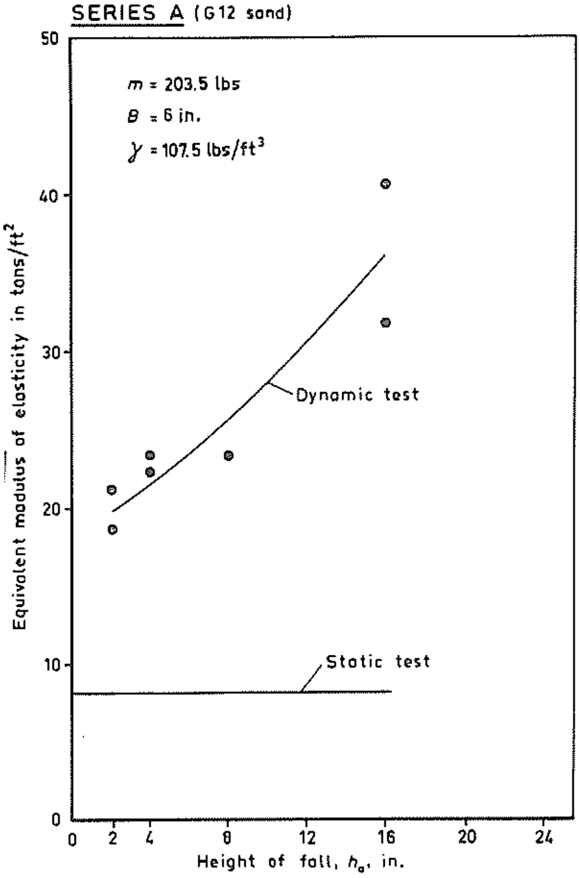

Fig. 16 Equivalent modulus of elasticity as a function of height of free fall. Test series A and 1

Retardation-time curves obtained from the field tests on Örsholm Sand (Test Series F) are shown in Fig. 14. Here only one maximum was obtained when the height of free fall was low (2 and 4 in.). When the height was increased to 8 or 16 in., two maxima were observed, the first occurred about 3 msec and the second about 5 msec after the weight struck the surface. The second retardation peak was probably also caused by reflection of the compression wave at the bottom of the sand layer (the average depth of the layer was approximately 10 ft). The calculated wave velocity is 885 ft/sec which is a higher value than that obtained at the laboratory tests. This can be attributed to differences in confining pressure in the sand in the two cases. (The thickness of the sand layer was 1.65 ft at the laboratory tests and about 10 ft at the field tests.) For still higher values of the height of free fall (8 or 16 in.) the second retardation peak was followed by a third not fully developed peak.

The measured dynamic and the corresponding static failure loads for test series F are shown in Fig. 17. Also here the dynamic failure load increased with increasing values of h_o.

The corresponding value of E_{eq}^{dyn} is shown in Fig. 18 as a function of h_o. The values are approximately constant when the height of free fall is small. A considerably larger value was obtained when h_o was increased to 16 in.

Plate Diameter (B). The effects of varying the plate diameter were investigated in test series B and G (Table 3). Typical retardation-time curves from these tests are shown in Figs. 19 and 20, where it can be seen that a height of free fall of 2 in. caused no interfering compression wave. Only one retardation peak was observed and its magnitude increased approximately linearly with increasing diameter of the bottom part of the weight.

The values of the dynamic failure loads obtained in test series B and the corresponding static loads are shown in Fig. 21 as a function of the plate diameter. As expected the dynamic failure loads increased with increasing plate diameter and the dynamic values were for the 2 in. plate approximately three times higher than the corresponding static values and were for the 6 in. plate approximately 50 % higher.

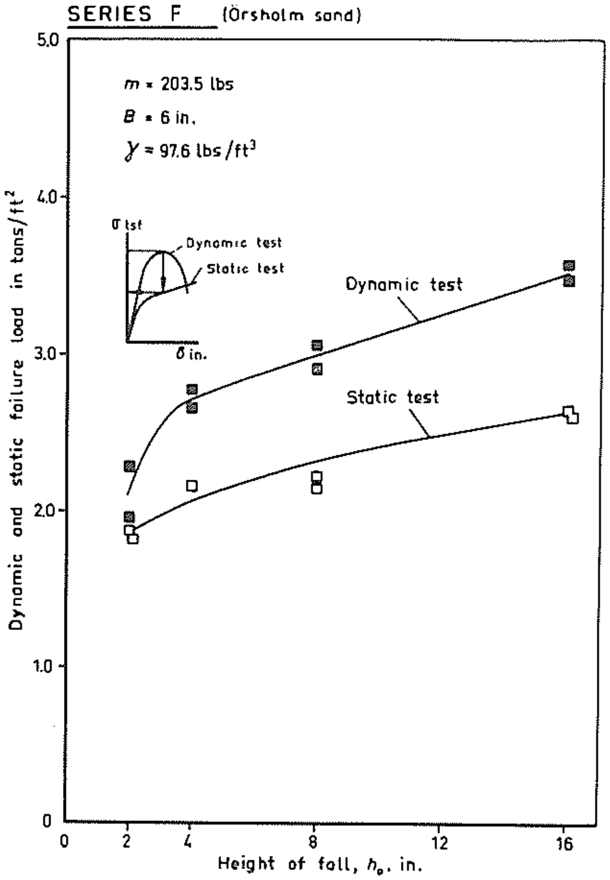

Fig. 17 Dynamic failure load as a function of height of free fall. Test series F and 7

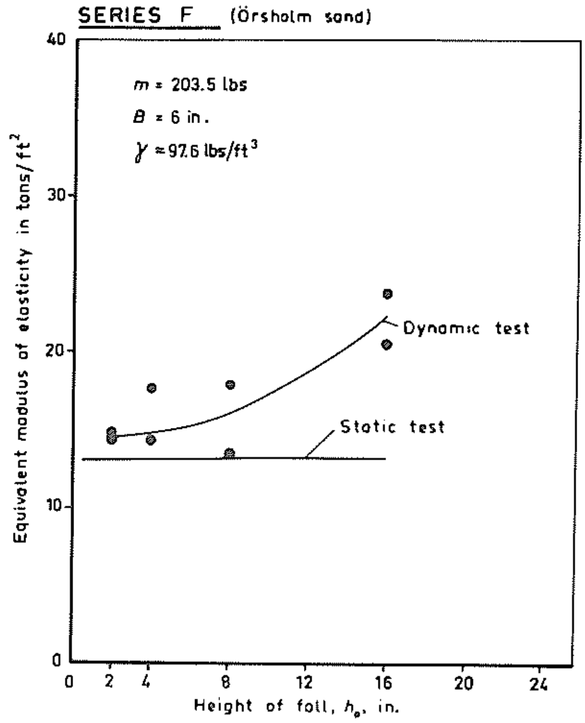

Fig. 18 Equivalent modulus of elasticity as a function of height of free fall. Test series F and 7

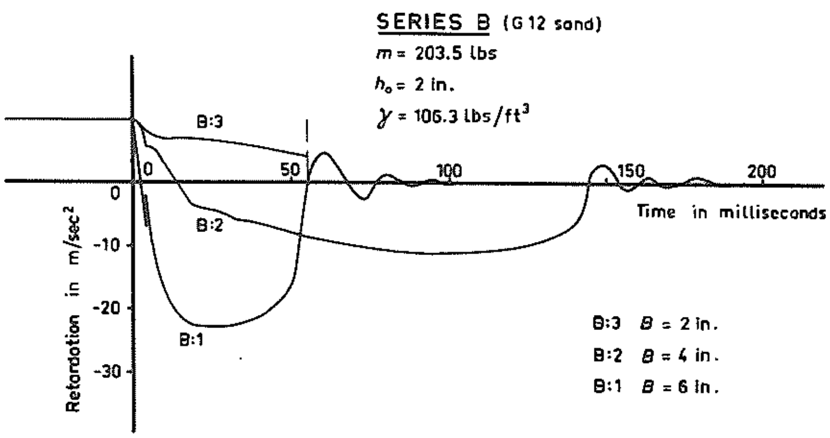

Fig. 19 Retardation-time curves from test series B

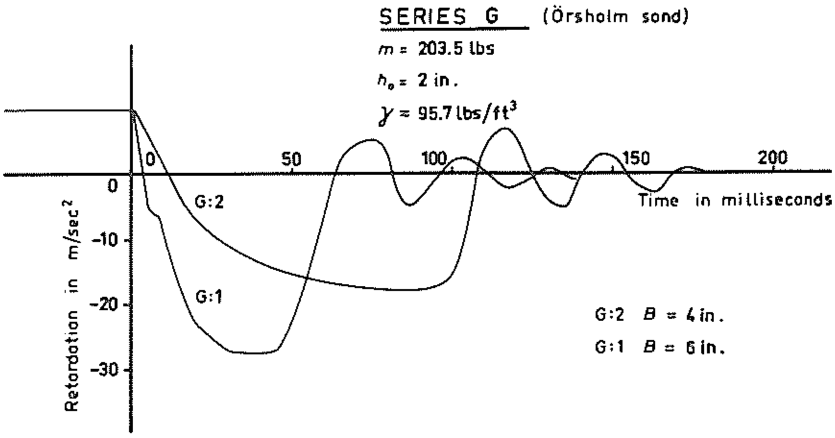

Fig. 20 Retardation-time curves from test series G

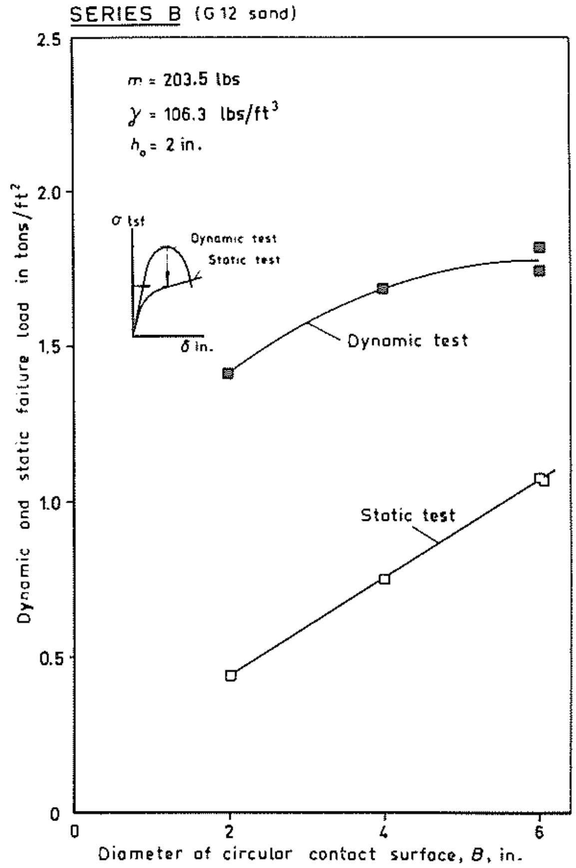

Fig. 21 Dynamic and static failure load as functions of plate diameter. Test series B and 2

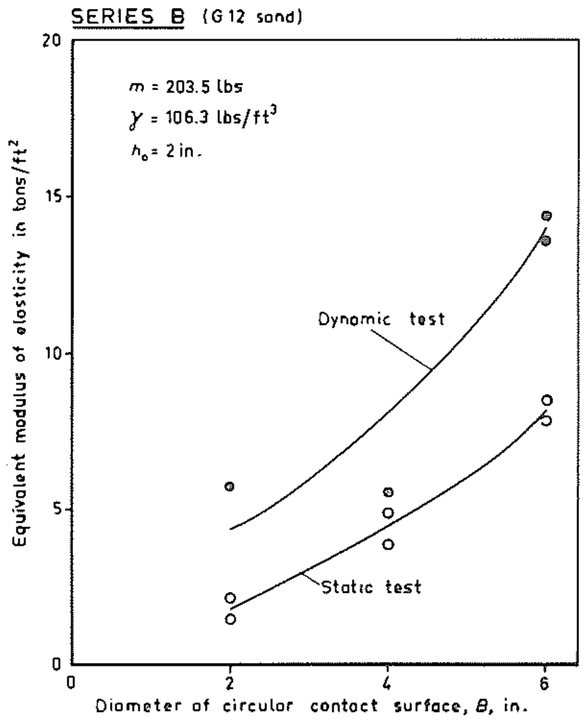

Fig. 22 Equivalent modulus of elasticity as a function of plate diameter. Test series B and 2

The values of E_{eq}^{dyn} obtained in test series B are shown in Fig. 22 together with the corresponding static values. The dynamic modulus was approximately twice the static values. Concerning the values of E_{eq}^{dyn} it is unavoidable that there will be some scatter of the test values, since a small inclination of the free-falling weight will appreciably affect the slope of the initial part of the load-settlement relationship on which the calculation of these values are based.

The retardation-time curves from test series G on the Örsholm Sand (Fig. 20) have approximately the same shape as those shown in Fig. 19. Also here the retardation peak increased with increasing plate diameter. The dynamic failure loads (Fig. 23) were also larger than the corresponding static loads. The difference was, however, smaller than at the laboratory tests on the G 12 Sand. Also the values of E_{eq}^{dyn} increased with increasing plate diameter as can be seen in Fig. 24.

Mass of Falling Weight (m). The effects obtained by varying the mass of the falling weight were investigated in tests on G 12 and Baskarp Sand (Table 3). The mass of the falling weight was 203.5, 428 and 1100 lbs, respectively, and the height of free fall and the diameter of the bottom surface of the weight were 2 and 6 in., respectively.

For the G 12 Sand tbe measured retardation-time curves (see Fig. 25) had only one retardation peak, while two peaks were observed for the Baskarp Sand (Fig. 26). The dynamic and the static failure loads obtained from these tests (Table 3) are compared in Figs. 27 and 28. It can be seen tbat the

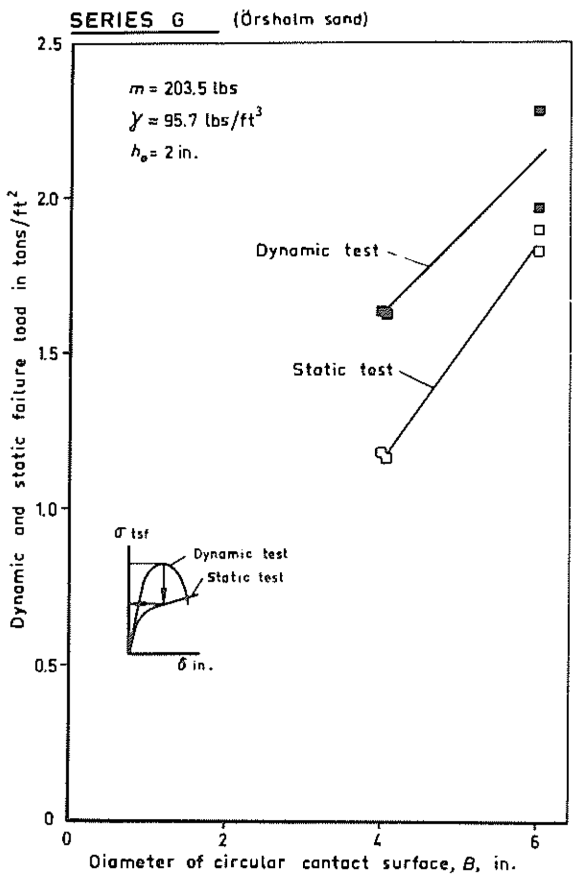

Fig. 23 Dynamic and static failure load as functions of plate diameter. Test series G and 7

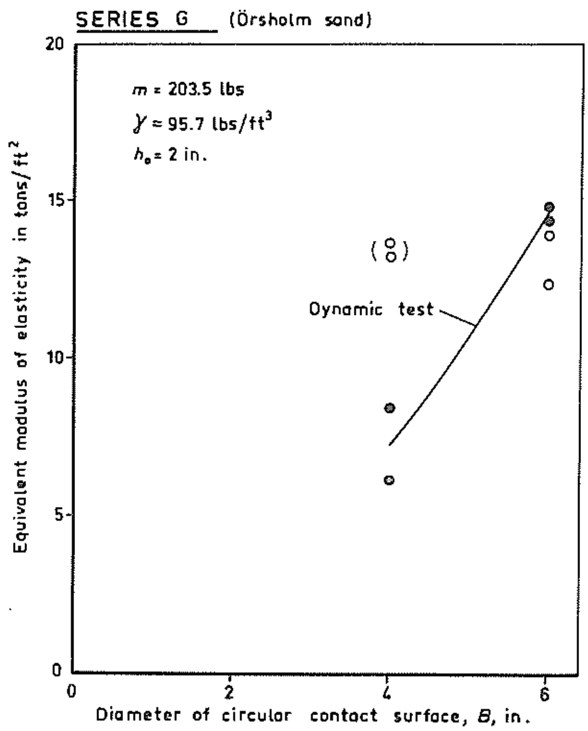

Fig. 24 Equivalent modulus of elasticity as a function of plate diameter. Test series G and 7

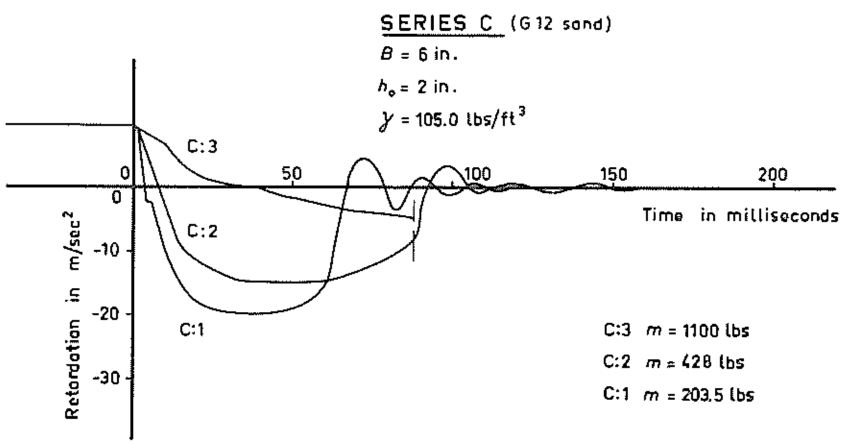

Fig. 25 Retardation-time curves from test series C:1, C:2 and C:3

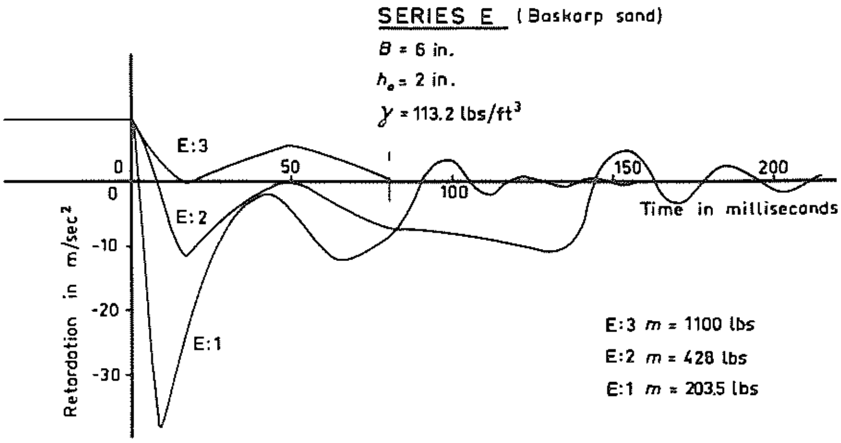

Fig. 26 Retardation-time curves from test series E:1, E:2 and E:3

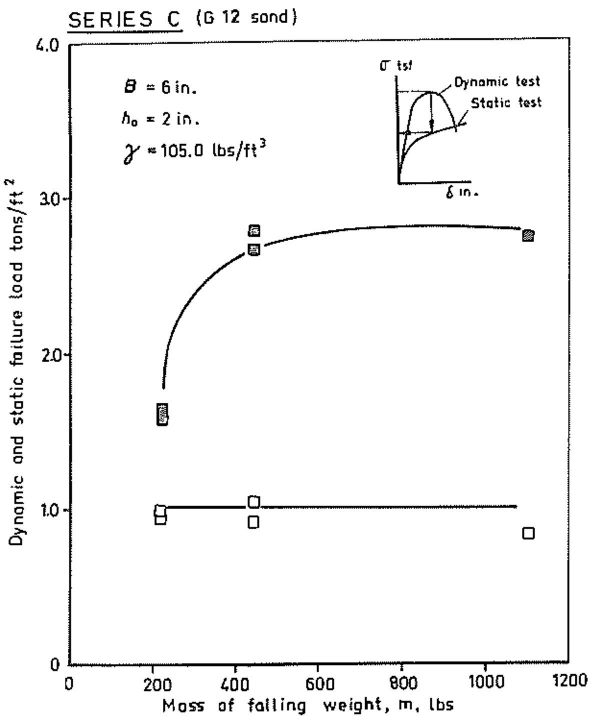

Fig. 27 Dynamic and static failure loads as a function of mass of falling weight. Test series C

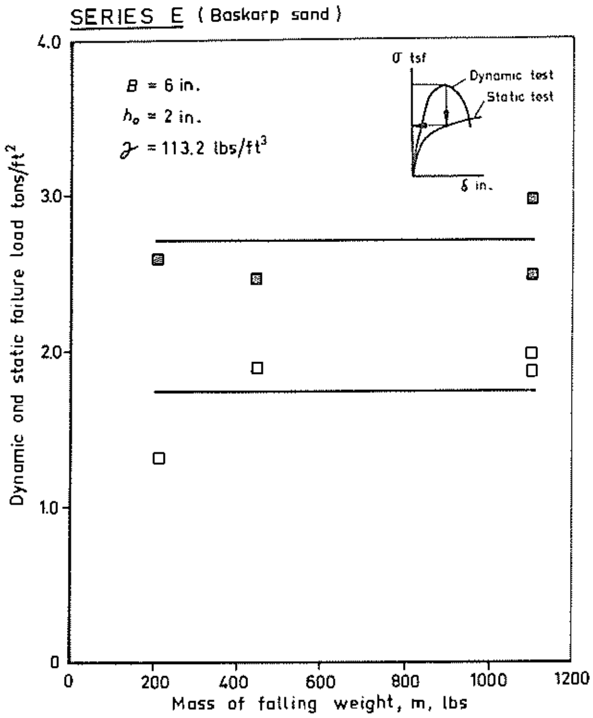

Fig. 28 Dynamic and static failure loads as a function of mass of falling weight. Test series E

dynamic loads were approximately 50 to 150 % larger than the corresponding static loads.

The experimentally determined values of E_{eq}^{dyn} are given in Table 3 and in Figs. 29 and 30 where also the static values are shown for comparisons. The values of E_{eq}^{dyn} are here approximately 100 % higher than the corresponding static values for the G 12 Sand, and approximately 50 % higher for the Baskarp Sand. The scatter of the individual test values was, however, rather large in these tests.

Unit Weight (γ). The influence of the unit weight of the sand and thus of the relative density was also investigated using the G 12 Sand (Table 3). The height of free fall and the diameter of the bottom plate of the weight were in these tests 2 in. and 6 in., respectively, Seven pairs of load tests were carried out with the 203.5 lbs weight. The observed retardation-time curves at different degree of compaction of the sand (γ = 101.5, 103.1, 103.8, 105.0, 106.2, 106.9 and 107.5 lb/ft^3) are illustrated in Fig. 31.

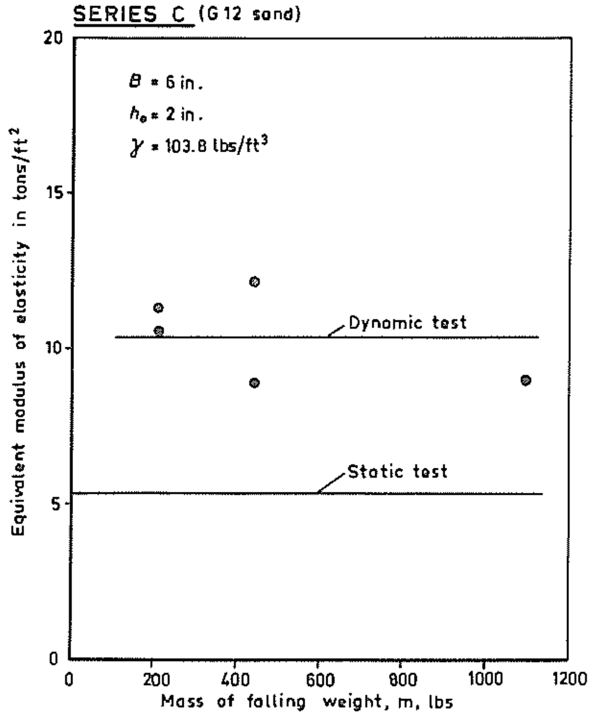

Fig. 29 Equivalent modulus of elasticity as a function of mass of falling weight. Test series C

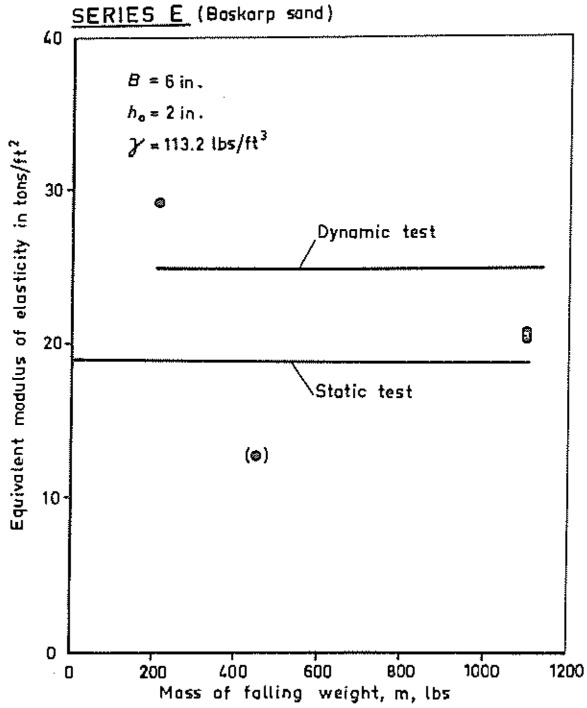

Fig. 30 Equivalent modulus of elasticity as a function of mass of falling weight. Test series E

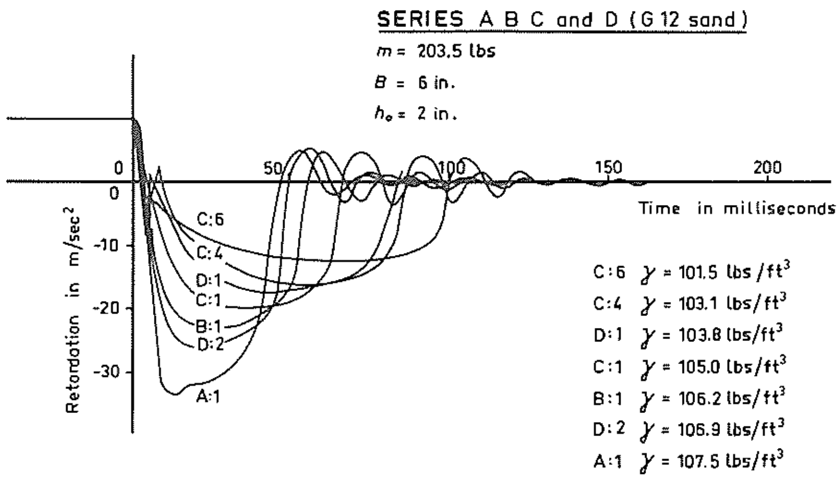

Fig. 31 Retardation-time curves from test series A, B, C and D

As can be seen the observed maximum retardations increased with increasing dry unit weight of the sand as also shown in Fig. 32 where the relationship between the retardation and the dry unit weight is approximately linear. In these tests the scatter of the individual test values was rather small, and it can be seen that the degree of compaction of the sand has a large influence on the measured maximum retardations and that the shape of the retardation-time curves changed appreciably by even small changes in the dry unit weight of the sand.

The dynamic and static failure loads are shown in Table 3 and Fig. 33 as a function of the dry unit weight. Both the dynamic and the static failure loads increased linearly with increasing dry unit weight. The dynamic failure load was for loose sand ($\gamma = 101.5$ lb/ft^3) approximately 40 % and for dense sand ($\gamma = 107.5$ lb/ft^3) approximately 70 % higher than the corresponding static values. It may be concluded from these results that a free falling weight can be used to check the relative density, or the degree of compaction of soils.

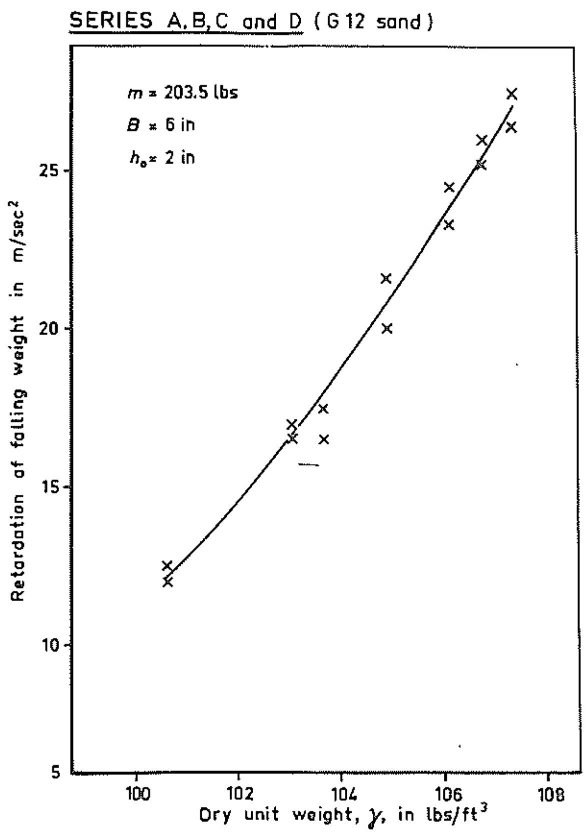

Fig. 32 Retardation of falling weight as a function of dry unit weight. Test series A, B, C and D

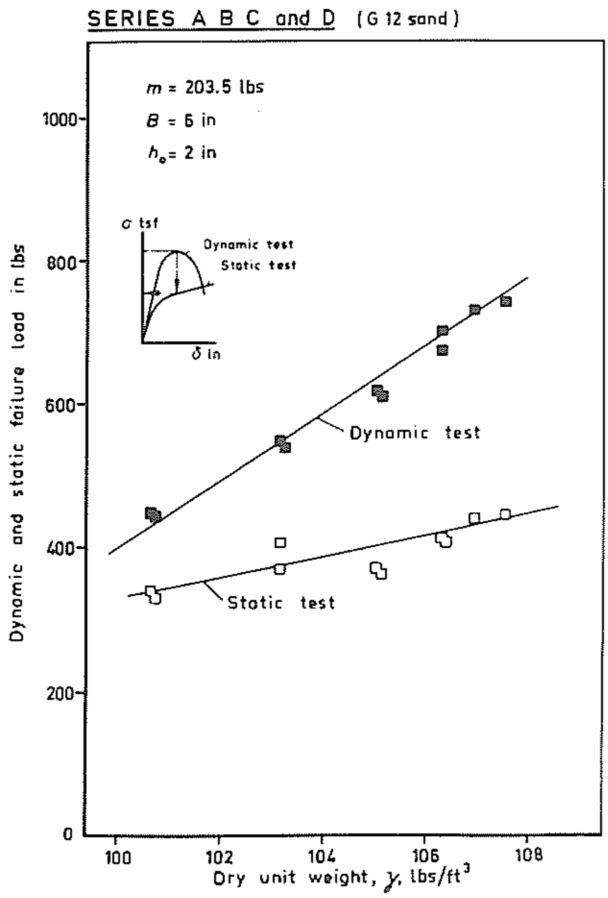

Fig. 33 Dynamic and static failure load as functions of dry unit weight. Test series A, B, C, D, 1, 2, 3, 4 and 5

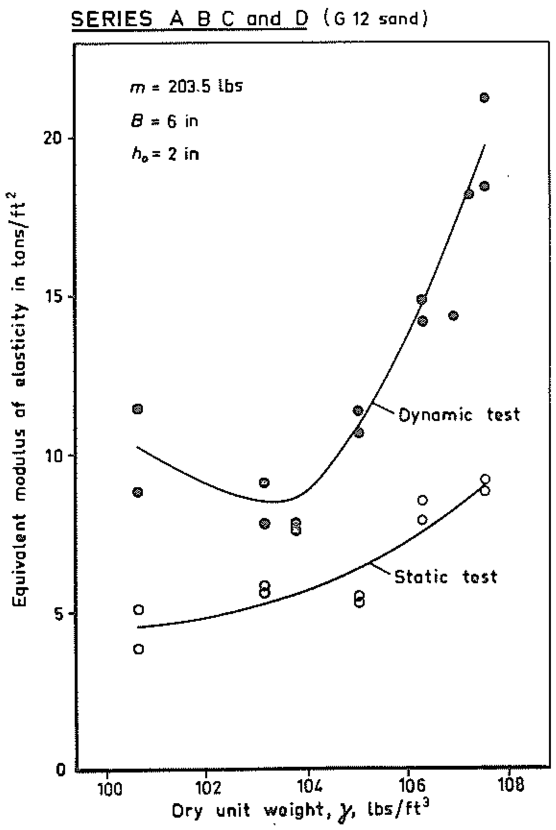

Fig. 34 Equivalent modulus of elasticity as a function of dry unit weight. Test series A, B, C, D, 1, 2, 3, 4 and 5

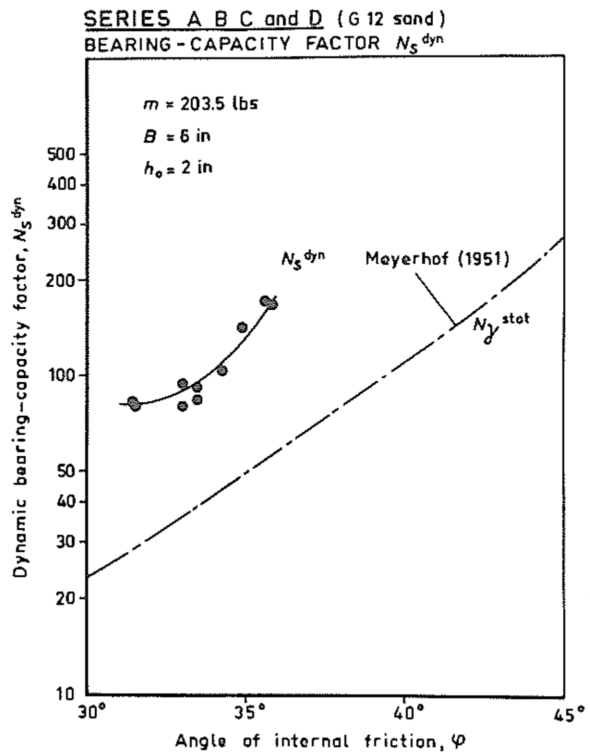

Fig. 35 Dynamic bearing capacity factor N_S^{dyn} as a function of φ.

In Fig. 34 it can be seen that the values of E^{dyn}_{eq} were approximately twice the corresponding static moduli and how both the dynamic and the static moduli increased with increasing degree of compaction. For the loosest compaction of the sand (γ = 101.5 lb/ft^3), the obtained dynamic moduli were, however, somewhat higher than the values for the medium dense sand (γ = 103.5 lb/ft^3). This difference can probably be explained by the fact that the values of E^{dyn}_{eq} were calculated from the initial part of the load-settlement curves which especially for loose sand is influenced by the surface phenomena discussed above.

The Bearing Capacity Factor N^{dyn}_{s}. The dynamic bearing-capacity factor N^{dyn}_{s}, calculated from series, A, B, and C on the G 12 Sand using Eq. (11) is shown in Fig. 35 as a function of the angle of internal friction of the sand. The angle φ was determined by usual triaxial tests on dry sand as mentioned above. It should be noticed that the friction angle is not appreciably affected by the loading rate as has been shown previously by e.g. Whitman & Healy (1962) and by Schimming, Haas & Saxe (1966). Whitman & Healy found that the angle of internal friction of three sands increased with less than 10 % when the time to failure decreased from five minutes to five milliseconds. Schimming, Haas & Saxe did not observe any rate effects in their direct shear tests on a coarse grained sand.

The measure values for N^{dyn}_{s}, shown in Fig. 35 are considerably higher than the theoretically calculated static values and also higher than experimentally determined static values.

6. MODES OF FAILURE IN SAND AT STATIC AND DYNAMIC LOAD TESTS

The dry unit weight of the sand was determined after each test below the loaded area at a depth of 5 and 10 in. The results are shown in Figs. 36 and 37 where each point represents the average of two measurements. These results show that different modes of failure occurred in the sand for tbe static and dynamic tests.

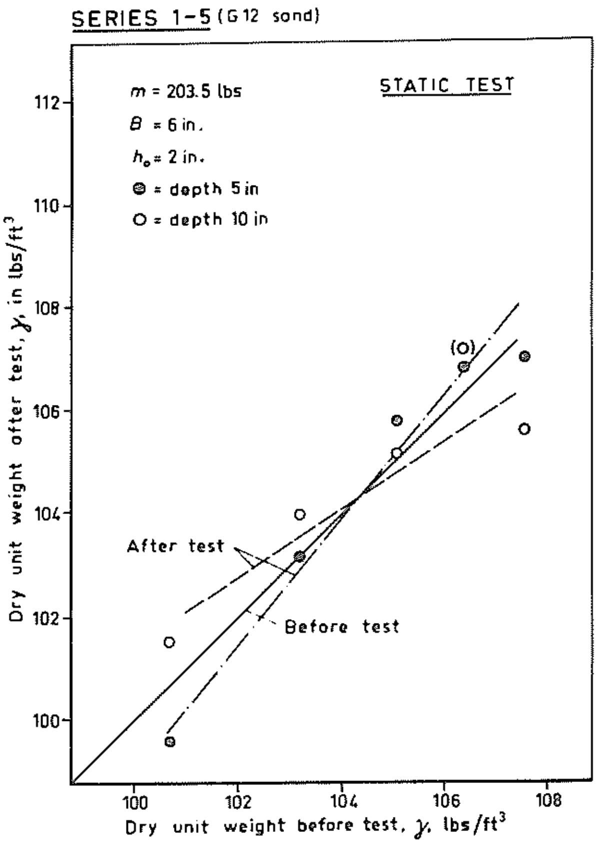

Fig. 36 Dry unit weight of G12 Sand before and after load test. Test series 1-5

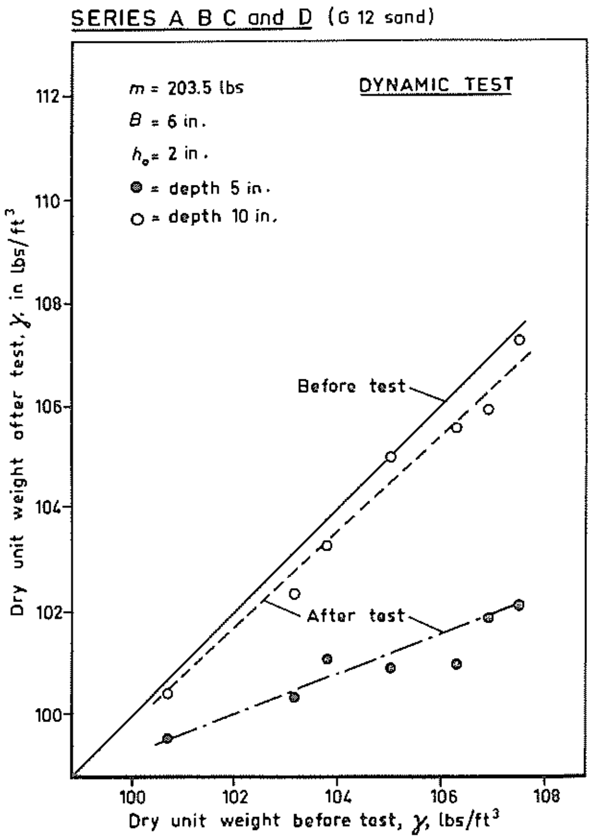

Fig. 37 Dry unit weight of G12 Sand before and after load test. Test series A, B, C and D

For the initially loose sand, as shown in Fig. 36, an increase of the unit weight was observed for the static tests at a depth of 10 in. below the surface, while the unit weight in this case decreased at the 5 in. level. For static tests on dense sand the unit weight was reduced at a depth of 10 in. below the surface while the change was small at a depth of 5 in.

At the dynamic tests on dense sand a large reduction of the unit weight occurred at the 5 in. level, while the reduction at the 10 in. level was small. For the dynamic tests the unit weight also decreased at the depth of 5 in. below the surface, while for test on initially loose sand, the unit weight was about constant at the 10 in. level.

7. CONCLUSIONS

Dynamic load-settlement relationships have been obtained by measuring the retardation of a free falling weight as a function of time when a weight strikes the surface of a soil mass. The tests indicate that the slope of the initial part of the dynamic load-settlement curves is steeper than the slope of the corresponding static curves and that the measured dynamic bearing-capacity was higher than the static bearing-capacity.

The measured dynamic load-settlement relationships were, especially for very loose sand disturbed by air which was trapped under the falling weight. This disturbance could be eliminated by scarifying the surface of the soil. The load-settlement relationships were also in some cases, especially for large heights, affected by reflection of the compression wave at the bottom of the soil layer. By reducing the height of free fall to 2 in. this effect could also be eliminated.

Effeets of Height of Free Fall. The dynamic failure loads increased by approximately 30 % when the height of free fall increased from 2 to 8 in. and by 20 % when the height increased from 8 to 16 in. Furthermore, the obtained dynamic failure loads from the laboratory tests on the G 12 and Baskarp Sands were about twice the static loads, measured at the same penetration depth, while for Örsholm Sand the difference was 30 %.

The dynamic equivalent modulus of elasticity also increased with increasing height of free fall and the values were for the laboratory tests approximately two to three times larger than the static values. At the field tests the difference between the dynamic and the static moduli, however, changed from 10 % to 80 % when the height of free fall increased from 2 to 8 in.

Effect of Plate Diameter. The measured dynamic failure loads also increased with increasing plate diameter. At a diameter of 2 in., the dynamic failure loads were for the G 12 Sand about three times the corresponding static values, and the corresponding difference for a plate diameter of 6 in. was 50%. At the field tests on Örsholm Sand the difference between the dynamic and the static failure loads, was 20 to 30 %.

The dynamic equivalent modulus of elasticity increased with increasing plate diameter and was for the laboratory tests 100 % higher than the corresponding static values.

Effect of Mass of Falling Weight. The measured dynamic failure loads also increased with increasing mass of the falling weight. These loads were for the laboratory tests twice the static values and the corresponding difference for the field tests was 25 %.

The equivalent modulus of elasticity was practically independent of the mass of the falling weight. For the laboratory tests on G 12 Sand the dynamic values were twice the static values, while for the field tests the difference was 20 %.

Effect of Degree of Compaction. Even small changes of the dry unit weight of the sand affected the test results appreciably. The maximum retardation increased linearly with increasing dry unit weight of the sand. Also the dynamic and the static failure loads increased linearly with increasing dry unit weight, while the dynamic failure loads for loose sand were approximately 40 % and for dense sand 70 % higher than the corresponding static loads. The test results thus indicate that a free falling weight can be used to check the relative density or the degree of compaction of sands.

Bearing Capacity Factors. Numerical values of the bearing-capacity factors N_q^{stat} and N_γ^{stat} were evaluated from the static load tests. The values were considerably higher than those theoretically calculated. The values of the bearing-capacity factor N_s^{dyn}, evaluated from the dynamic tests were 50 to 100% higher than the bearing-capacity factors N_q^{stat} or N_γ^{stat} from the static load tests.

REFERENCES

BISHOP, A.W., 1966. The strength of soils as engineering materials. Sixth Rankine Lecture. Géotechnique Vol. 16 No. 2 p. 91-130.

CHRISTENSEN, N.H., 1961. Model tests on plane active earth pressures in sand. Danish Geot. Inst. Bull. No. 10. Copenhagen.

CORNFORTH, D.H., 1964. Some experiments on the influence of strain conditions on the strength of sand. Géotechnique Vol. 14 No. 2 p. 143-167.

CUNNY, R.W. & SLOAN, R.C., 1961. Dynamic loading machine and results of preliminary small-scale footing tests. ASTM Spec. Techn. Publ. No. 305 p. 65-77.

DE BEER, E.E. & VESIĆ, A., 1958. Étude expérimentale de la capacité portante du sable sous des fondations directes établies en surface. Ann. Trav. Publ. Belgique No. 3. 54 p.

DE BEER, E.E. & LADANYI, B., 1961. Étude expérimentale de la capacité portante du sable sous des fondations circulaires établies en surface. Proc. 5. Int. Conf. Soil Mech. a. Found. Engng. Vol. 1 p. 577-585.

FEDA, J., 1961. Research on the bearing capacity of loose soil. Proc. 5. Int. Conf. Soil Mech. a. Found. Engng. Vol. 1 p. 635-642.

FISHER, W.E., 1962. Experimental studies of dynamically loaded footings on sand. Ph. D. Thesis Univ. of Ill. Urbana USA.

FORSSBLAD, L., 1963. Jordvibreringsundersökningar. Stockholm.

FORSSBLAD, L., 1965. Investigations of soil compaction by vibration. Acta Polytechnica Scandinavica. Ci 34. p. 85-111.

FORSSBLAD, L., 1967. Dynamic load-bearing tests by falling weight. Inform. Bull. Dyn. Test. of Roads a. Runways No. 6. Shell. Amsterdam.

HANSEN, B., 1961. The bearing capacity of sand tested by loading circular plates. Proc. 5. Int. Conf. Soil Mech. a. Found. Engng. Vol. 1 p. 659-664.

HANSEN, B. & ODGAARD, D., 1960. Bearing capacity tests on circular plates on sand. Danish Geot. Inst. Bull. No. 8. Copenhagen.

HARDIN, B.O. & RICHART, F.E., Elastic wave velocities in granular soils. J. Soil Mech. a. Found. Div. Proc. ASCE Vol. 89 No. SM1 p. 33-65.

LAWRENCE, F.V., 1961. Laboratory measurement dilatational wave propagation velocity. MIT Dep. Civ. Engng. Rep. R 63-8.

LUNDGREN, H. & MORTENSEN, K., 1953. Determination by the theory of plasticity of the bearing capacity of continuous footings on sand. Proc. 3. Int. Conf. Soil Mech. a. Found. Engng. Vol. 1 p. 409-412.

MEYERHOF, G.G., 1951. The ultimate bearing capacity of foundations. Géotechnique Vol. 2 No. 4. p. 301-332.

MUHS, H., 1954. Ergebnisse von Probebelastungen auf grossen Lastflächen zur Ermittlung der Bruchlast im Sand. Fortschr. u. Fortsch. Bauw. Reihe D H. 17 p. 57-82.

MUHS, H., 1959. Neuere Entwicklung der Untersuchung und Berechnung von Flachfundationen. Mitt. Deutsch. Forsch. ges. Bodenmech. (Degebo) H. 13. p. 1-15.

MUHS, H., 1963. Über die zulässige Belastung nichtbindiger Böden. Mitt. Deutsch. Forsch. ges. Bodenmech. (Degebo) H. 16 p. 103-121.

ORRJE, O., 1968. Dynamic loading tests on cohesionless soils with free falling weights, compared with static plate loading tests. Div. of Soil Mech. Royal Inst. of Techn. Stockholm.

SCHIMMING, B. B., HAAS, H.J. & SAXE, H.C., 1966. Study of dynamic and static failure envelopes. J. Soil Mech. a. Found. Div. Proc. ASCE Vol. 92 No. M2 p. 105-124.

SCHULTZE, E., 1955. Aussprache zum Vortrage Dipl.-Ing. Kahl. Deutsch. Ges. Erd-u. Grundb. e.V., Vorträge der Baugrundtagung 1954 in Stuttgart p. 56-64.

SELIG, E.T. & Mc KEE, K.E., 1961. Static and dynamic behavior of small footings. J. Soil Mech. a. Found. Div. Proc. ASCE Vol. 87 No. SM 6 p. 29-47.

SHENKMAN, S. & Mc KEE, K.E., 1961. Bearing capacities of dynamically loaded footings. ASTM Spec. Techn. Publ. No. 305 p. 78-90.

TAYLOR, D.W. & WHITMAN, R.V., 1954. The behavior of soils under dynamic loadings. 3. Final report on laboratory studies. MIT Dep. Civ. Sanit. Engng. Rep. AFSWP-118.

TERZAGHI, K., 1943. Theoretical soil mechanics. New York p. 118-129.

TERZAGHI, K., 1955. Evaluation of coefficients of subgrade reaction. Géotechnique Vol. 5 No. 4 p. 297-326.

VESIĆ, A., 1963. Bearing capacity of deep foundations in sand. Highw. Res. Rec. No. 39 p. 112-153.

VESIĆ, A., BANKS, D.C. & WOODARD, J.M., 1965. An experimental study of dynamic bearing capacity of footings on sand. Proc. 6. Int. Conf. Soil Mech. a. Found. Engng. Vol. 2 p. 209-213.

WHITE, C.R., 1964. Static and dynamic plate-bearing tests on dry sand without overburden. U.S. Naval. Civ. Engng. Lab. Techn. Rep. No. R 277. Port Hueneme, California.

WHITMAN, R.V. & HEALY, K.A., 1962. Shear strength of sands during rapid loadings. J. Soil Mech. a. Found. Div. Proc. ASCE Vol. 88 No. SM 2 p. 99-132.

WHITMAN, R.V. & LAWRENCE, F.V., 1963. Discussion on: Elastic wave velocities in granular soils. J. Soil Mech. a. Found. Div. Proc. ASCE Vol. 89 No. SM 5 p. 112-118.

LIST OF PROCEEDINGS OF THE SWEDISH GEOTECHNICAL INSTITUTE